2.5. Seiche

An evaluation of the seiche flood hazard at MPS was performed. Two surface water bodies at MPS have been identified as requiring evaluation, including: 1) the Long Island Sound and 2) the discharge basin (former quarry). Tsunami-induced seiche is discussed in Section 2.6.

2.5.1. Method

Seiche at MPS was evaluated with consideration of meteorological, astronomical, and seismic forcing as the causative mechanism for low frequency water surface oscillations or seiche in Long Island Sound and the discharge basin. The hierarchical-hazard assessment approach (HHA) described in NUREG/CR-7046 (NRC, 2011) was applied at MPS to determine whether a seiche in either Long Island Sound or the cooling water discharge basin (former quarry) could result in a significant flooding event.

The initial step is the determination of the natural period of oscillation in each water body. The period is estimated analytically and verified by observations where available. Next the period of each external forcing mechanism is examined as a possible driver of the system. Amplification of surface height oscillations can occur when the forcing period is close to the natural period of the basin, a phenomena known as resonance. If resonance is possible, further analysis of observed water level data is used to characterize the response to forcing in the basin. If the observed response is strongly damped then the flooding risk posed by the PMS is mitigated.

Based on the configuration of the water bodies that have the potential to impact MPS, Merian's Formula was used to evaluate both semi-enclosed and enclosed basins. For semi-enclosed basins, Merian's Formula is based on a one-quarter-wavelength standing wave (see Figure 2.5-1 for definitions). The primary seiche mode for a semi-enclosed basin can be estimated using Merian's Formula as follows (Scheffner, 2008 and Rabinovich, 2009):

$$T = \frac{4l}{(1+2n)\sqrt{gh}} \qquad \text{(Equation 1)}$$

where:

T is the period (seconds)
l is the length of the basin (feet)
g is the acceleration due to gravity (feet per square second)
h is the average depth of the basin (feet)
$\sqrt{gh}$ is the shallow water wave speed
n = the number of nodes along the axis of the basin (0 for the primary mode of a semi-enclosed basin), n=0,1,2...

For an enclosed basin the standing wave is reflected at both ends and thus the system has two anti-nodes. The node in an enclosed system is located at the midpoint of the basin, see Figure 2.5-1. Merian's Formula for an enclosed basin is Equation 2 below (Scheffner, 2008 and Rabinovich, 2009):

$$T = \frac{2l}{n\sqrt{gh}} \qquad \text{(Equation 2)}$$

where:

T is the period (seconds)
l is the length of the basin (feet)
g is the acceleration due to gravity (feet per square seconds)
h is the average depth of the basin (feet)
$\sqrt{gh}$ is the shallow water wave speed
n = the number of nodes along the axis of the basin, 1 for the primary mode in an enclosed basin

2.5.2. Results

2.5.2.1. Long Island Sound

Long Island Sound is approximately 150 kilometers in length and 30 kilometers in width at its widest point with an average depth of 79 feet (Signell et al 1997). The Sound has a roughly ellipsoidal shape narrowing at the western and eastern ends. The sound connects to the New York Harbor at the western end via the East River (Figure 2.5-1). The tides in the East River and the Sound are out of phase and decoupled, driving a strong current through the East River, but they are not a significant source of tidal energy to Long Island Sound. At the eastern end of the Sound, an island chain runs between Orient Point on Long Island and Napatree Point, Rhode Island, defining the southeastern extent of Long Island Sound and the boundary between it and adjacent Block Island Sound to the east (Figure 2.5-1). There is a large deep channel ("The Race") between Little Gull Island and Fishers Island that is the primary source of tidal forcing in Long Island Sound at the western end. The eastern end of Long Island Sound is the node of the longitudinal seiche mode while the western end at Throgs Neck is the anti-node. It is also possible for the basin to support transverse seiche modes across its width.

Meteorological, astronomical, and seismic forcing can all cause waves in an estuary such as Long Island Sound. However, for seiche to pose a risk to the MPS, the forcing period must be at the natural frequency of the basin. Merian's Formula predicts a seiche period of 9.6 hours in the longitudinal direction and 0.4 to 0.9 hours in the transverse direction based on the geographic parameters of the Sound (Table 2.5-1).

Earthquakes: The typical frequency content of earthquakes falls outside the range of the estimated natural period of Long Island. Resonance within Long Island Sound will not occur due to the difference in the natural period of the Sound and the typical range of ground motion (shaking) periods from earthquakes which typically do not exceed 10 seconds (Chung et al., 2008).

Meteorological: Meteorological forcing has a much broader energy spectrum. While there is a significant wind driven circulation in Long Island Sound, periodic forcing capable of generating a seiche is not possible. At small scales local convection drives wind gusts with a period of about one minute (Wells, 1997). Diurnal heating and cooling also drive relatively weak periodic motions. These weak periodic motions are associated with typical wind speed variability, which is on the order of 13 feet per second at night and 26 feet per second during the day (Svensson et al., 2010). This variation occurs daily, and has shown to pose no threats to MPS. Finally, in temperate regions, there is a high energy band at the synoptic scale. The period of synoptic variability in the atmosphere is typically on the order of 100 hours (Wells, 1997). The synoptic scale is the spatial and temporal scale of temperate weather systems, which in the United

States is about 3 to 7 days (Wells, 1997). Of these only the synoptic scale forcing or periodic storms are sufficient to cause significant water level changes in Long Island Sound. However the period of the synoptic variability is too long to force a seiche in the basin. A single storm might cause a large storm surge; however, to drive a resonant response greater than the initial surge, the storm would have to be repeated approximately twice per day. Storms and other atmospheric phenomena are not forcing mechanisms that would persist over many cycles with a constant period (Wells, 1997)

Waves: Wind generated wave periods which can range from 4 to 20 seconds (Wells, 1997), and are too short to drive a resonant seiche in the longitudinal or transverse directions in Long Island.

Astronomical: The semi-diurnal tide does exhibit a significant resonant amplification in the western end of Long Island Sound (NOAA, 2012). However the observations confirm that there is no threat to MPS, which is at the eastern end of the basin near the node of the longitudinal basin oscillation. There is no evidence of tidal forcing for a transverse seiche mode in the water level data near MPS. The frequency predicted by linear theory is too high for diurnal and semi-diurnal resonance.

2.5.2.2. Discharge Basin

The Millstone Point Quarry (Figure 2.5-2) was opened to Long Island to become the cooling water discharge basin for MPS. This small, deep basin could potentially support longitudinal or transverse seiche modes.

The natural period of oscillation for the discharge basin was calculated using Merian's formula for both the longitudinal and transverse modes. The fundamental mode of the basin is the primary concern as it is the least damped mode. In the longitudinal direction the basin is a semi-enclosed mode bounded at the north end by the quarry wall and open at the south end to Long Island Sound. In the transverse direction the basin is enclosed, bounded by the east and west walls of the quarry. The longitudinal seiche period was estimated at 83.3 to 92.5 seconds and the transverse seiche period is estimated at 6.9 to 12.1 seconds.

Earthquakes: The frequency content of earthquakes can vary by earthquake and by the distance of the site from the earthquake epicenter (and amount of damping that occurs); however, the frequency content is typically less than 10 seconds (Chung et al., 2008). The period of the primary mode of the discharge basin (83 to 93 seconds) in the longitudinal direction is not within the typical range of ground motion (shaking) periods. Resonant seiching in the transverse direction within the discharge basin will not impact MPS since the transverse sides of the discharge basin consist of the remains of the prior quarry operation or are undeveloped (Figure 2.5-2). The areas along the transverse sides of the discharge canal slope back to Niantic Bay and Long Island and therefore, water overtopping of the transverse sides of the basin will flow back to Long Island Sound.

Meteorological: While meteorological and hydrodynamic phenomena do exist with frequencies in this range, they are generally weak and not capable of forcing a seiche mode in the discharge basin. Wind gusts can have a spectral peak near one minute (Wells, 1997) but over the relatively short, protected fetch in the quarry it is not possible to cause a significant surface height disturbance

Waves: Wind generated wave periods which can range from 4 to 20 seconds are too short to drive a resonant seiche in the longitudinal direction (Wells, 1997). Further, the small cross section of the canal decouples the discharge basin from the surface height oscillations in Long Island preventing surface gravity waves from driving a seiche. In the transverse direction the Discharge Basin is too narrow and sheltered by the surrounding grades to allow the generation of wind waves.

Astronomical: The astronomical tides in the Long Island Sound have periods that are several orders of magnitude larger than the longitudinal period of the discharge basin and will not cause resonance.

2.5.3. Conclusions

Seiche poses no flood risk to MPS based on the screening analysis performed using Merian's formula and literature review. No further analysis or modeling is necessary.

2.5.4. References

2.5.4-1 **Chung et al., 2008.** "Seismic Resistance Capacity of High-Rise Buildings subjected to Long-Period Ground Motions – E – Defense Shaking Table Test, The 14th World Conference on Earthquake Engineering," Beijing, China, October 2008.

2.5.4-2 **NOAA, 2012.** National Oceanic and Atmospheric Administration Historic Water Level Data: Six Minute Water Level. Kings Point NY (Station 8516945), Bridgeport CT (Station 8467150), New Haven CT (Station 8465705), New London CT (Station 8461490), and Montauk (Station 8510560).

2.5.4-3 **NRC, 2011.** "Design Basis Flood Estimation for Site Characterization at Nuclear Power Plants - NUREG/CR-7046", U.S. Nuclear Regulatory Commission, November 2011.

2.5.4-4 **Rabinovich, 2009**. "Seiches and Harbor Oscillations." In: Kim, Y.C. ed. Handbook of Coastal and Ocean Engineering. World Scientific, Singapore, 2009, 193–236.

2.5.4-5 **Scheffner, 2008**. "Water Levels and Long Waves." In: Demirbilek, Z., Coastal Engineering Manual, Part II, Coastal Hydrodynamics Chapter 5-6, Engineer Manual 1110-2- 1100, U.S. Army Corps of Engineers, Washington, D.C.

2.5.4-6 **Signell et al., 1997.** Signell, R.P., Knebel, H.J., List, J.H., and Farris, A. (1997) Physical Processes Affecting the Sedimentary Environments of Long Island Sound. In M.L. Spaulding and A.F. Blumberg (Ed.), 5th International Conference on Estuarine and Coastal Modeling (pp. 400 - 412). Alexandria, Virginia: American Society of Civil Engineers (ASCE).

2.5.4-7 **Svensson et al., 2010**. Svensson, G. et al., Evaluation of the Diurnal Cycle in the Atmospheric Boundary Layer Over Land as Represented by a Variety of Single-Column Models: The Second GABLS Experiment, March 2010.

2.5.4-8 **Wells, 1997.** Wells, N. "The Atmosphere and Ocean, A Physical Introduction." John Wiley & Sons Ltd, 1997.

Table 2.5-1: Parameters for length, depth and resulting period of the fundamental seiche mode for Long Island Sound

End Points	Length	Depth	Basin Type	Period (hours)
New Rochelle to Block Island Sound	486,962 feet (148,419m)	98 feet (30 m)	semi-enclosed	9.6
Millstone Point to Plum Island	41,423 feet (12,625 m)	115 feet (35 m)	enclosed	0.4
Millstone to Montauk	101,275 feet (30,867 m)	115 feet (35 m)	enclosed	0.9

Note: Since the basin is irregularly shaped, a range of representative lengths is used to calculate the possible seiche period.

Figure 2.5-1: Overview of Long Island Sound and location of MPS relative to the Sound. ("The Race" is highlighted by the red box.)

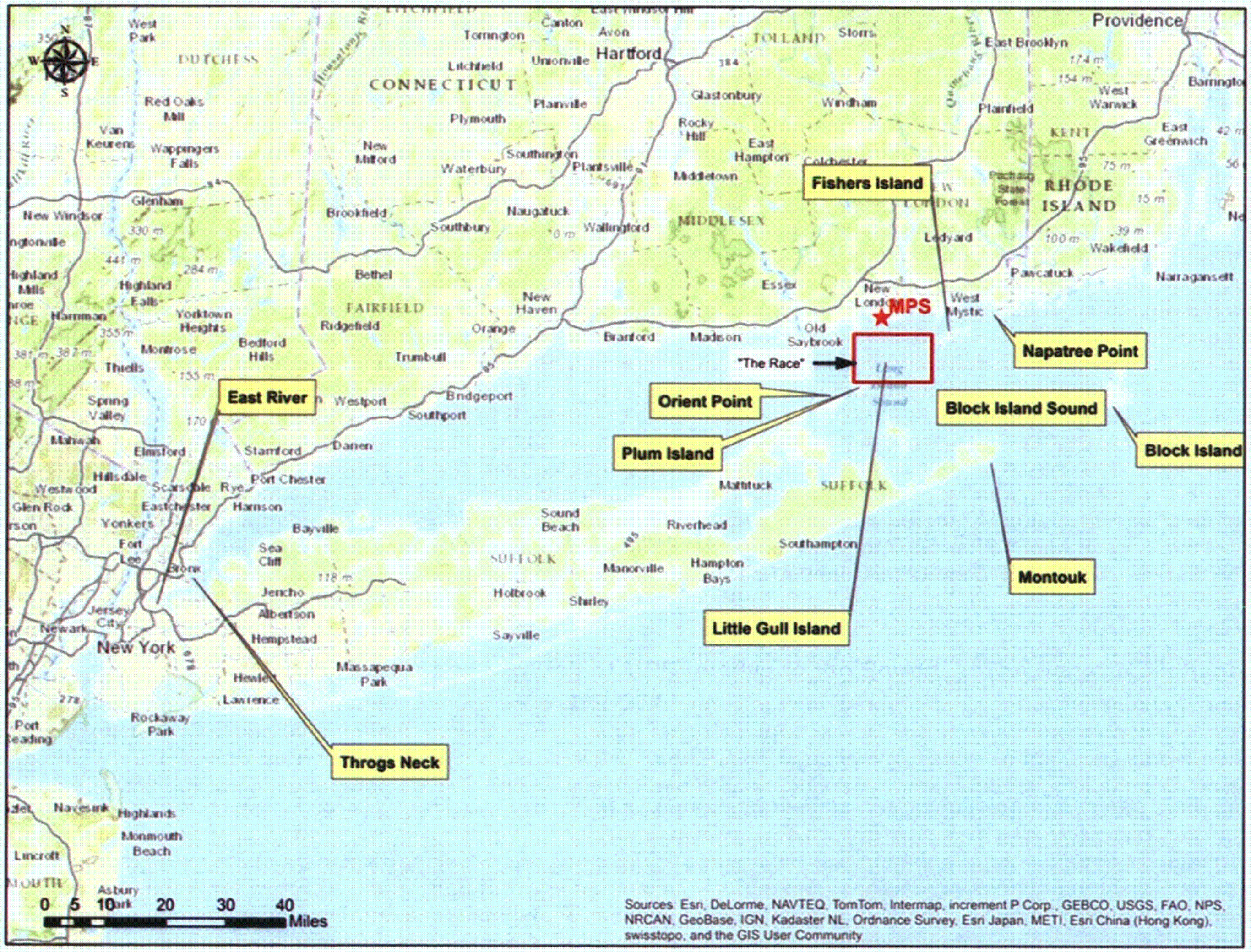

Figure 2.5-2: MPS site from satellite image showing Millstone Point and the location of the discharge basin in the old Millstone quarry

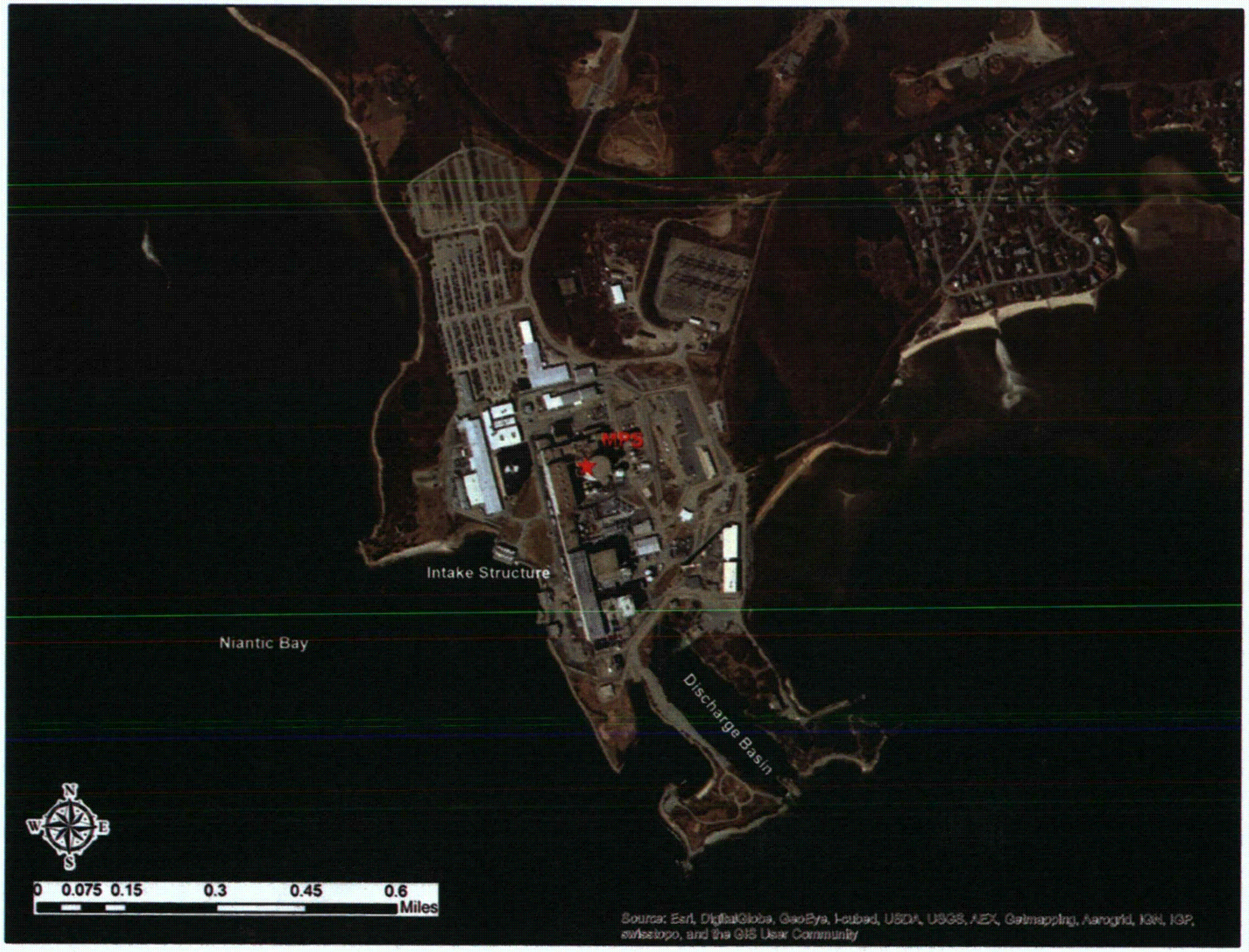

2.6. Tsunami

This section evaluates the Probable Maximum Tsunami (PMT) at MPS. Due to its proximity to the Atlantic Ocean, MPS is considered a coastal site potentially subject to oceanic tsunamis.

2.6.1. Method

Along the U.S. East Coast, a number of potential near- and far-field tsunami sources have been identified, which are caused by various geophysical processes, including earthquakes (i.e., co-seismic events), and submarine or subaerial landslides (NOAA, 2012a).

First, a screening test was performed based on literature review. The results of the MPS regional tsunami screening test indicate a region of potential tsunami hazard near MPS in eastern Long Island Sound. The screening test identifies four sources with the potential to cause significant tsunamis in the region, which include:

1. An extreme co-seismic tsunami (M9.0) generated in the Caribbean Subduction Zone (Puerto Rican Trench).
2. An extreme co-seismic tsunami (M9.0) generated within the Azores-Gibraltar Convergence Zone similar to the 1755 Lisbon earthquake.
3. A subaerial landslide representing an extreme flank failure (450 km^3) at the Cumbre Vieja Volcano in the Canary Islands.
4. A near-field extreme submarine mass failure similar to the Currituck historical case, which is used as a proxy for the largest possible submarine mass failure (SMF) in the area. The Currituck event was a translational landslide that occurred along the continental margin off the coast of Virginia and North Carolina between 22,500 and 43,300 years ago (Grilli et al., 2011). It is considered to be one of the largest submarine landslides to have occurred off the U.S. East coast.

For the re-evaluation, parameters for these four sources have been updated based on the most recent tsunami inundation modeling along the U.S. East Coast done for the National Tsunami Hazard Mitigation Program (NTHMP), which is summarized as follows:

1. <u>Puerto Rice Trench (PRT) M9 co-seismic source</u>: As part of recent NTHMP work, several PRT parameters were revised slightly, including the number and locations of sub-sources and the earthquake magnitude (from M8.9 to M9) (Grilli et al, 2013a).

2. <u>Lisbon M9 co-seismic source:</u> The Lisbon source was reanalyzed in recent NTHMP analysis (Grilli et al, 2013b). Because there is considerable uncertainty in the parameters of this historical source (particularly the strike angle), the NTHMP analysis modeled a number of possible sources to determine worst case impacts along the upper U.S. East Coast. In total, 16 different scenarios at different strike angles all with a M9 magnitude were simulated. The scenario with the worst case impact for the upper U.S. East Coast was identified in the NTHMP and used as the "worst case" scenario herein.

3. <u>Cumbre Vieja Volcano (CVV) 450 km^3 subaerial landslide source</u>: For this analysis the results of the detailed three-dimensional (3D) modeling work (Abadie et al., 2012) are used to specify the tsunami source. As part of recent NTHMP analysis, detailed

inundation modeling from this source was performed for selected areas of the U.S. East Coast (Grilli et al., 2013c). The same source propagation methodology is used herein.

4. Currituck SMF proxy: A detailed analysis of the historical Currituck submarine landslide, in combination with recent geotechnical and geological analyses (some performed as a collaboration between the University of Rhode Island (URI) and the United States Geological Survey [USGS]) identified four areas between Virginia and Massachusetts with elevated tsunami risk (Grilli et al., 2013d). A SMF Currituck proxy source was parameterized for each of these areas. The location designated as Area 2 is located directly offshore MPS and the SMF parameters developed for this area are used herein.

The completion of a site screening test, required as a next step by the hierarchal hazard assessment (HHA) approach presented in NUREG/CR-6966 (NRC, 2011), is precluded by the complex geography of the region, particularly the deep and wide channels that connect Long Island Sound to the Atlantic Ocean. Therefore, a modeling approach that incorporates the complex geography of Long Island Sound was used. The methodology includes the following steps:

1. Definition of the antecedent water levels in the vicinity of MPS—the 10-percent exceedance high tide (e.g., high tide level that is equaled or exceeded by 10 percent of the maximum monthly tides over a continuous period).
2. Parameterization of the 3 far-field and 1 near-field tsunami sources.
3. Simulation of tsunami generation, propagation, and inundation in a series of nested grids (Table 2.6-1) ranging from a 1 minute spherical grid (in deep water) to a 10 meter Cartesian grid (in the immediate vicinity of MPS). Simulations of the tsunamigenic sources were performed using a combination of the Fully Nonlinear Boussinesq Wave Model with TVD Solver (FUNWAVE-TVD) and the Non-Hydrostatic Wave Model (NHWAVE) computer models. FUNWAVE-TVD is a fully nonlinear and dispersive Boussinesq long wave model used to propagate tsunami waves and quantify inundation and drawdown. NHWAVE is a three-dimensional, sigma coordinate non-hydrostatic model used to compute the SMF tsunami source.
4. Generation of maps and time-series graphs describing tsunami impacts at MPS.
5. Analysis of the model sensitivity to changes in local topography.
6. Estimation of drawdown due to each tsunamigenic source using Green's Law.

Computational modeling of tsunamis was performed by subject matter expert, Dr. Stéphan Grilli, PhD, P.E. of the University of Rhode Island.

2.6.2. Results

2.6.2.1. Antecedent Water Level

In accordance with ANSI/ANS-2.8-1992 (ANSI, 1992), the 10-percent exceedance high tide can be determined from recorded tide data or from predicted astronomical tide tables. NOAA maintains a secondary tidal prediction station in the vicinity of MPS at Watch Hill, RI (Station 8458694, NOAA, 2013a). This station is located along Block Island Sound just east of MPS (Figure 2.6-1). The Watch Hill station has a documented offset coefficient from Newport, RI (NOAA, 2013b). This offset is used to convert the 10 percent exceedance high tide elevation calculated for Newport to the Watch Hill station. The 10 percent exceedance high tide at Watch Hill is representative of the 10 percent exceedance high tide at the open coast nearest MPS. The NOAA station in Newport, RI has a period of record 1943-2012 of verified monthly water levels. Once the monthly high tide data was sorted and ranked, the Weibull plotting position was used to calculate the exceedance probability for each high tide value in the table. The Weibull plotting position equation was applied as follows:

$$Pe = 100\left(\frac{m}{(n+1)}\right)$$

where:

Pe = the probability of exceedance
m = rank
n = total number of monthly high tide values

The 10 percent exceedance high tide at Newport, RI was calculated to be 3.67 feet NAVD88. This value was then multiplied by an offset conversion factor of 0.74 to Watch Hill, RI. The resultant 10 percent exceedance high tide at Watch Hill, RI was calculated to be 2.7 feet NAVD88.

The final step is to the addition of sea level rise to the 10 percent exceedance high tide. Historic sea level rise trends in the vicinity of MPS are available for the Montauk, NY NOAA station (NOAA, 2013c). The long term sea level rise rate of 0.13 in/year (3.20 mm/year) at Montauk is based on monthly sea level data from 1947 to 2011. This gives an expected 50-year sea level rise rate of 0.5 feet. The resultant 10 percent exceedance high tide used as input to the FUNWAVE-TVD model was therefore 3.2 feet NAVD88, equivalent to 4.2 feet MSL.

2.6.2.2. Tsunami Source Parameters

Puerto Rican Trench M9

The Caribbean subduction zone is a source of large earthquakes that could potentially cause an extreme tsunami impacting the U.S. East Coast and thus MPS. For this evaluation, an extreme M9 co-seismic source from the Puerto Rico Trench is defined using a combination of 12 NOAA Short-term Inundation Forecast for Tsunamis (SIFT) M7.5 unit sources. Altogether, these sources cover a 600 km by 100 km area. To account for the greater magnitude (M9), assuming a moderately shallow rupture and a shear modulus equal to 45 GPa (for subducting material), a slip of 14.8 meters is defined for each of the sub-faults (Grilli et al., 2010). This approach to parameterizing the PRT source is similar to recent modeling carried out as a part of the NTHMP (Grilli et al., 2013a).

The initial tsunami elevation for this source was derived using the Okada method (Okada, 1985). The Okada method is an analytical solution for a semi-infinite homogeneous medium (the seafloor) with a dislocation specified along an oblique plane. The maximum seafloor deformation predicted by this solution was specified as a hot start on the free surface (due to the near incompressibility of water and small rise time). The initial water velocity was set to zero for initializing the simulation of this source. The resulting initial sea surface amplitude used for modeling ranges from about -20 feet to +26 feet. This source was re-interpolated in the 1 arc-minute grid and used to perform basin scale propagation simulations with FUNWAVE-TVD as described in Section 2.6.2.3.

Far-Field Co-Seismic Tsunami – Lisbon M9

The Azores-Gibraltar plate boundary (a.k.a., Azores convergence zone) is another possible source of earthquakes that could cause an extreme tsunami impacting the U.S. East Coast. There are numerous potentially active faults within the convergence zone, including the Gorringe Bank Fault, the Marque de Pombal Fault, the St. Vincente Fault, and the Horseshoe fault. It is not clear which faults are presently active in the region; however, these faults, collectively, are considered to be the source of some of the largest historical earthquakes and tsunamis in the Atlantic Ocean, including the M8.5-8.9 1755 Great Lisbon Earthquake and tsunami (Grilli et al., 2011).

The Lisbon Earthquake was reanalyzed in the recent NTHMP work (Grilli et al., 2013b) because of uncertainty in the source parameters, particularly the strike angle. To determine the worst case impact for the upper U.S. East Coast, 16 scenarios were simulated at different strike angles, each having a M9 magnitude. The scenario with the maximum impacts for the upper U.S. East Coast was selected as the source for this evaluation and is known as "Source Area 1, Case 5" in the NTHMP work. Source Area 1 is located in the region west of the Madeira Tore Rise (Figure 2.6-2). It has a 15 degree strike angle and a 20 meter slip, with a depth of 5 kilometers, length of 317 kilometers, width of 126 kilometers, dip of 40 degrees, and a rake of 90 degrees (Grilli et al., 2013b).

The initial sea surface elevation ranges from -7 feet (-2 meters) to +33 feet (+10 meter) using Okada's method. This source was re-interpolated in the 1 arc-minute grid and used to perform basin-scale propagation simulations with FUNWAVE-TVD as described in Section 2.6.2.3.

Far-Field Subaerial Landslide - Cumbre Vieja Volcano

A complete flank collapse of the Cumbre Vieja Volcano (CVV) on La Palma, in the Canary Islands (Figure 2.6-3), is another potential source of an extreme tsunami that could impact the U.S. East Coast. The tsunami source corresponding to the extreme flank collapse of the CVV considered by Abadie et al. 2012 as their worst case (a 450 km^3 volume) was used to initialize FUNWAVE-TVD. The initial surface elevation and current velocities for this source were computed by Abadie et al. 2012. After filtering and depth integration, these results were specified in FUNWAVE-TVD to simulate propagation across the Atlantic Ocean.

Propagation was performed initially in the region around La Palma using a 500 meter Cartesian grid (Grilli et al., 2013c). At about 20 minutes after initiation, waves are directed toward the west-northwest (i.e. towards the upper U.S. East Coast) and have amplitudes ranging from -50 meters to +50 meters (-164 feet to +164 feet). This source was re-interpolated in the 1 arc-minute grid and used to perform basin scale propagation simulations with FUNWAVE-TVD as described in Section 2.6.2.3.

Near-Field Submarine Mass Failure

The most notable submarine landslide complex along the continental margin adjacent to the U.S. East Coast is known as the Currituck landslide. It is considered the largest SMF known to have occurred along the U.S. East Coast. The landslide occurred about 100 kilometers off of the coast of Virginia and North Carolina between 22,500 and 43,300 years ago (Grilli et al., 2011 and Locat et al., 2009). It was likely a single event caused by an earthquake, although two separate large failures that likely failed in sequence were identified. The SMF down-slope length was about 30 kilometers, the width about 20 kilometers, and the maximum thickness varied between 250-750 meters (ten Brink et al., 2008).

The area located directly southwest of Ryan Canyon and almost directly offshore from the mouth of Long Island Sound (and thus directly offshore from MPS) was identified in recent NTHMP work (Grilli et al., 2013d) as one of four locations between Virginia and Massachusetts at elevated risk to tsunamis generated by SMFs (Figure 2.6-4).

The NTHMP work parameterized a SMF Currituck proxy for what is known as "Area 2" in the recent NTHMP work (Grilli et al., 2013d). The parameters used are summarized in Table 2.6-2. The SMF is assumed to have a Gaussian shape and a total volume of about 135 cubic kilometers.

2.6.2.3. Model Grid Inputs

The governing equations in FUNWAVE-TVD are discretized on a regular grid, either spherical or Cartesian. A nested gridding scheme is implemented to allow for higher spatial resolution of the model near the tsunami sources and the coastline(s) being studied. The gridding scheme is based on a one-way coupling method, which works by computing time series of free surface elevation and currents in the coarser grid, for a large number of numerical gauges (stations) defined along the boundary of the finer grid. Computations in the finer nested grid are then performed using these time series as boundary conditions. Two formulations of equations in different coordinate systems are used in FUNWAVE-TVD – one in spherical coordinates, which includes Coriolis effects, but is only weakly nonlinear in its current implementation (Kirby et al., 2013); the other in Cartesian coordinates, which is fully nonlinear, but is only valid for smaller, local or regional grids due to the earth curvature (Shi et al., 2012). The first coordinate system is used for early stages of long-distance propagation of a potential tsunami over oceanic scales, and the latter is used for calculating regional propagation and coastal impact.

Each source, with the exception of the SMF, is initialized on a 1 arc-minute spherical grid. The SMF source is initialized on a Cartesian grid at higher resolution (approximately 500 meters) given the close proximity of the source event to MPS. As indicated before, and further described below, a series of increasingly higher-resolution grids are "nested" within FUNWAVE-TVD to transition from the full model extent to areas of very fine resolution (approximately 10 meter by 10 meter grid) near MPS. The gridding approach used by FUNWAVE-TVD generally increases resolution from one grid to the next by a factor of 3 to 4; this is as a typical range that has been found in earlier work to ensure good accuracy and convergence of the nested simulations (Grilli et al., 2013a; Grilli et al., 2013b; Grilli et al., 2013d). NHWAVE is a non-hydrostatic wave model and is used to compute tsunami generation from the near-field (SMF) source. The geometry and kinematics of the SMF are modeled and specified as bottom boundary conditions in the model. NHWAVE solves Euler equations in a "sigma-layer" 3D discretization. Results are reported at four stations near MPS (Table 2.6-3; also see Figure 2.6-5).

Bathymetry and topography were interpolated in each model grid from a variety of sources, including:

1. NOAA's 1 arc-minute resolution ETOPO-1 database (obtained from gravitational anomaly and reconciled with coastal relief models in shallower water) (Amante et al., 2009).
2. 1/3 arc-minute (approximately 90 meter) resolution National Geophysical Data Center (NGDC) Coastal Relief Model (CRM), which extends in the northeast from the coastal zone to the continental shelf (NOAA, 2013d).
3. 1/3 arc-second (approximately 10 meter) resolution NTHMP Montauk DEM (Eakins et al., 2009) combined with 1-meter 2012 Post Sandy USACE LiDAR data (NOAA, 2012b).

In addition, near-field simulations of the CVV source, which was found to provide the most flooding at the site (CVV; see below for details) and of the PRT source, were performed at the two finest levels of nesting. Both the original Montauk DEM and a revised version, updated to include LiDAR elevation data collected after Hurricane Sandy in October, 2012, were used.

As discussed above, four initial tsunami waves were generated based on the specific physics of each tsunami source, using a relevant model (e.g., co-seismic sources using Okada's method, landslide sources directly modeled with full 3D models based on source kinematics). Each initial tsunami source was then propagated with FUNWAVE-TVD, in a series of nested grids of increasing resolution, from 1 arc-minute resolution down to 10 meters near the MPS site. Table 2.6-4 describes the grid dimensions and stations used as boundary conditions for each of the far-field source model grids; Table 2.6-5 lists comparable parameters for the near-field source grids.

Modeling of bottom friction and breaking dissipation in incident wave trains is of prime importance in the higher resolution (nearshore) grids. In all model grids a bottom friction coefficient for coarse sand of 0.0025 was used; this is conservative since friction is typically larger nearshore and onshore. Wave breaking is modeled in FUNWAVE-TVD by using a breaking criterion (set to surface elevation equal to 0.8 times the local depth in this case) to detect areas of breaking events and then disabling dispersive terms in these areas (Shi et al., 2012). The threshold for wetting/drying of model grid cells was set to 1 centimeter.

2.6.2.4. Model Simulations for the Maximum Probable Tsunami

Results of the detailed tsunami modeling calculation at MPS are summarized below. For each source, the initial propagation of the wave and the overall features of the generated tsunami at or near the shelf break are discussed in terms of surface amplitudes and wavelength of the leading wave. Detailed modeling results, such as runup and inundation at MPS, are presented for the finest (10 meter) grid that surrounds the site. In some cases, predictions of inundation from coarser grids are presented to confirm the relevance and accuracy of simulations. Inundation levels from FUNWAVE-TVD and NHWAVE in the figures are presented in meters above the antecedent water level of 3.2 feet NAVD88.

For each source event, maps of the maximum inundation (runup) levels resulting from FUNWAVE-TVD simulations are calculated. In addition, time series of water surface elevations were output from each model run at four numerical gauges in the vicinity of MPS (Figure 2.6-5; Table 2.6-3). Gauge locations in Niantic Bay and Long Island Sound were selected to visualize the time series of tsunami arrival near MPS at a range of water depths. In all cases, similar results were observed at each station due to the large (spatial) wavelength characteristics of the incoming tsunami.

PRT M9 co-seismic source

Figure 2.6-6 shows instantaneous surface elevations computed in the 1 arc-minute grid after 30, 102, and 200 minutes (3.33 hours) of propagation, as well as the maximum computed surface elevation within each grid cell over the duration of the model run. Although the initial amplitude of the tsunami wave generated from the PRT source ranges from -6 meters to +8 meters (-20 feet to +26 feet, see Figure 2.6-7), directional spreading and propagation over the wide U.S. East Coast shelf leads to large reductions in the waves' amplitudes prior to reaching the MPS site.

The maximum water surface elevation along the western side of the site is approximately 3.21 meters above the antecedent water level, which is equivalent to 14.7 feet MSL. As shown in Figures 2.6-8 and 2.6-9, this predicted water level elevation inundates the undeveloped area northwest of MPS3. Ground elevations in this area and near the MPS paved parking lot are around 30.0 feet MSL, providing a natural barrier to the safety related structures at the southern end of the site from flooding from the northwest area. Further south, the maximum water surface elevations at MPS2 and MPS3 are 8.6 feet MSL. On the eastern side of the site, the maximum water surface elevation reaches 9.8 feet MSL.

Lisbon M9 co-seismic source

As with the PRT source, large reductions in the waves' amplitudes occur as they propagate through the basin and across the continental shelf. While the initial tsunami wave ranges from -2 meters to +10 meters (-6.6 feet to 32.8 feet, see Figure 2.6-10), by the time the wave reaches the 100 meter isobaths along the U.S. East Coast the amplitudes range from -0.98 feet to 0.98 feet (Figure 2.6-11). This reduction is shown through time series of surface elevations computed previously and summarized in Grilli et al., 2013b.

Due to the general direction, substantial directional energy spreading, and the dissipation across the shelf, only minor inundation is predicted at the MPS site. The initial tsunami wave arrives in the vicinity of MPS approximately 5.5 hours after the source event. As shown in Figures 2.6-12 and 2.6-13, the maximum water surface elevations occur east of the site, although results do not vary substantially on either side of the peninsula. Elevations at the stations range between -0.13 feet to 0.26 feet (Figure 2.6-14). The maximum water surface elevations east of MPS reach only 4.6 feet MSL.

Cumbre Vieja Volcano 450 km^3 subaerial landslide source

Figure 2.6-15 shows time series of tsunami elevations computed at a series of stations at the 200 meter isobath along the U.S. East Coast. At this depth, the leading tsunami wave from the CVV source arrives at the shelf south of MPS approximately 6.5 hours after the event and has about a -20 feet trough and +16.5 feet elevation, with about a 24 minute period. The initial tsunami is followed by a series of smaller waves, approximately -9.8 feet to +9.8 feet in amplitude.

Near-field inundation maps computed in finer resolution grids (Figures 2.6-16 through 2.6-19) indicate that the CVV source produces the largest impact at MPS among the modeled far-field sources. The water surface elevations become gradually amplified as they approach MPS. Time series are shown in Figure 2.6-20.

The maximum flood elevation along the western side of the site is approximately 21.1 feet MSL. Ground elevations in this area and near the MPS paved parking lot are around 30.0 feet MSL, providing a natural barrier to the safety related structures at the southern end of the site from flooding from the northwest area. This water level elevation causes inundation in the undeveloped coastal area northwest of MPS3 (west of the parking lots). The maximum water surface elevations further south, near MPS2 reach 14.7 feet MSL. On the eastern side of MPS, the maximum water surface elevation reaches 12.0 feet MSL.

The tsunami resulting from an extreme flank failure of the CVV requires approximately 6.5 hours to propagate across the North Atlantic basin to the continental shelf break and approximately 2.0 hours to travel from the shelf break to MPS. Maximum runup levels are predicted to occur 8.7 hours after this source event.

Near-Field Submarine Mass Failure

As shown in Figure 2.6-21, the SMF Currituck proxy source produces initial surface waves with amplitudes between -49 feet to +49 feet. As with the other sources listed above, the tsunami undergoes significant reduction in amplitude as the waves propagate over the shelf and into Long Island Sound due to both directional energy spreading and bottom friction. Figure 2.6-22 and Figure 2.6-23 shows the envelope of maximum water surface elevations computed for the SMF Currituck proxy source in the vicinity of MPS in the 30- and 10- meter grids respectively. Both grids predict that maximum wave heights will be less than 7 feet for areas south of MPS; however, surface elevations are amplified within the embankments on either side of the peninsula.

Figure 2.6-24 shows water surface elevations computed at all four stations in the 10- meter grid. The SMF tsunami wave is predicted to arrive in the vicinity of MPS approximately 2 hours after the source event. At these locations, water surface elevations computed by the FUNWAVE-TVD model range between -0.9 feet to +7.2 feet. As shown in Figure 2.6-25, the SMF source results in inundation around the perimeter of the site. The extent of this inundation is most pronounced in the undeveloped area northwest of MPS3, where the maximum water surface elevation is approximately 15.1 feet MSL. Ground elevations in this area and near the MPS parking lot are around 30.0 feet MSL, providing a natural barrier to the safety related structures at the southern end of the site from flooding from the northwest area. The maximum water surface elevations further south, adjacent to MPS2 were 10.3 feet MSL. On the eastern side of the site, the maximum water surface elevation reaches 10.6 feet MSL.

2.6.2.5. Low Water Drawdown Due to Tsunami

Drawdown from the four tsunamigenic sources during the 90 percent low tide were estimated using Green's Law. Green's law states that the amplitude of the tsunami is proportional to the square root of the square root of the ocean depth (Dean et al., 1990). This relationship can be modified as the ocean depth varies as follows:

$$A_2 \sim A_1 \left[\frac{h_1}{h_2}\right]^{\frac{1}{4}}$$

Where:

A_2 = Maximum low tide tsunami drawdown at Station 2 (ft)

A_1 = Maximum high tide tsunami drawdown at Station 2 (ft)

h_1 = depth at Station 2 based on the 10 percent exceedance high tide (ft)

h_2 = depth at Station 2 based on the 90 percent low tide (ft)

The 90 percent low tide is defined as the low tide level that is equal to or less than 90 percent of the minimum monthly tides over a continuous period (e.g., 10 percent of low tides are below this value). The 90 percent low tide is calculated by:

1. Statistical analysis of recorded tide data from the NOAA Newport, RI (Station 8452660) CO-OPS station, which is located approximately 50 miles east from MPS using the Weibull plotting position equation.

2. Conversion of the Newport, RI 90 percent low tide to the Watch Hill 90 percent low tide. This offset is used to convert the 90 percent low tide elevation calculated for Newport to the Watch Hill station. The 90 percent low tide at Watch Hill is representative of the 90 percent low tide inside Long Island Sound near MPS.

Because Green's law is a simplified approach and long waves (i.e. tsunamis) are not sensitive to local changes in depth, Station 2 is considered applicable to approximate drawdown at the MPS intake. Furthermore, Station 2 is located approximately a half mile offshore from the MPS intake, where a tsunami wave would have minimal time to adjust to the varying bathymetry directly offshore from the intake and is thus an appropriate location to estimate local drawdown.

The depth at Station 2 was determined from the Montauk, NY 1/3 arc–second Mean High Water DEM (Eakins et al., 2009). Once the depth at the intake structure was determined, each tide elevation was converted to a relative depth to be used in Green's Law.

The maximum drawdown at low tide is a result of the PRT M9 co-seismic source, resulting in a maximum drawdown of -1.05 feet below the 90 percent low tide antecedent water level of -1.79 feet MSL at Station 2. The total drawdown elevation is therefore -2.84 feet MSL.

2.6.2.6. Tsunami-induced Seiche Potential

Computer simulations for all tsunamigenic sources were performed for adequate durations to capture (if any) tsunami induced seiche motion. Since the dominant seiche period in Long Island Sound is 0.4 hours (see Section 2.5) the tsunami impact at MPS has been computed (solving the full equations in the time domain for the actual geometry and bathymetry of the site area) for several periods. Hence, if seiches were to occur as a result of the incident tsunami in the transverse direction off MPS, seiching oscillations would have been triggered in the modeling and their effect is already present in the model results. Once the tsunami forcing stops, if seiching modes exist, they will continue to oscillate but with gradually reducing amplitude due to dissipation by friction. The results for all tsunamigenic sources indicate that a seiche will not occur due to the PMT.

2.6.3. Conclusions

A detailed tsunami hazard assessment was conducted to identify applicable near-field and far-field tsunami sources and model wave propagation to the nearshore and inundation at MPS. Four potential tsunamigenic sources were identified: (a) a M9 earthquake that ruptures the PRT, (b) a M9 earthquake occurring at the Azores-Gibraltar convergence zone, (c) an extreme flank collapse of the CVV, and (d) a SMF on the continental slope directly south of the site. A summary of the results is presented in Table 2.6-6.

Simulations of wave propagation and inundation for each tsunamigenic source were performed on a series of nested grids using the FUNWAVE-TVD model. Inputs for modeling each of the simulations were based on existing published (and peer-reviewed) research. For the near-field (SMF) source, the NHWAVE model was used to first compute the water levels and currents based on slide motion. The generated waves were then propagated toward the coastline at MPS using FUNWAVE-TVD.

For all cases, substantial reductions in the initial wave heights are predicted due to directional energy spreading during propagation from the source to the site, dissipation from bottom friction over the wide shelf, and wave breaking in shallow water areas. The highest predicted runup elevations in the vicinity of MPS result from the subaerial landslide (extreme flank failure) of the CVV. Propagation of the initial CVV surface waves across the Atlantic Ocean and into Long Island Sound results in maximum water levels of approximately 14.7 feet MSL near MPS.

2.6.4. References

2.6.4-1 **Abadie et al, 2012.** Abadie, S., J. C. Harris, S. T. Grilli, and R. Fabre. (2012). Numerical modeling of tsunami waves generated by the flank collapse of the Cumbre Vieja Volcano (La Palma, Canary Islands): tsunami source and near field effects. J. Geophys. Res., 117, C05030, doi:10.1029/2011JC007646.

2.6.4-2 **Amante et al., 2009**. Amante, C. & Eakins, B.W. (2009). ETOPO1 1 arc-minute global relief model: Procedures, data sources, and analysis (19 p.). NOAA Technical Memorandum NESDIS NGDC-24.

2.6.4-3 **ANSI, 1992.** American National Standards Institute/American Nuclear Society. (1992). *ANSI/ANS-2.8-1992: Determining Design Basis Flooding at Power Reactor Sites.*

2.6.4-4 **Dean et al., 1990**. Dean, R.G. and Dalrymple, R.A. (1990): Water Wave Mechanics for Engineers and Scientists. Singapore, World Scientific, Advanced Series on Ocean Engineering, Vol 2.

2.6.4-5 **Eakins et al., 2009**. Eakins, B.W., L.A. Taylor, K.S. Carignan, R.R. Warnken, T. Sazonova, D.C. Schoolcraft. (2009). Digital Elevation Model of Montauk, New York: Procedures, Data Sources, and Analysis, NOAA Technical Memorandum NESDIS NGDC-17, National Geophysical Data Center, Marine Geology and Geophysics Division, Boulder, CO.

2.6.4-6 **Grilli et al., 2010**. Grilli, S.T., S. Dubosq, N. Pophet, Y. Pérignon, J.T. Kirby and F. Shi. (2010). Numerical simulation and first-order hazard analysis of large co-seismic tsunamis generated in the Puerto Rico trench: near-field impact on the North shore of Puerto Rico and far-field impact on the US East Coast. Natural Hazards and Earth System Sciences, 10, 2109-2125, doi:10.5194/nhess-2109-2010.

2.6.4-7 **Grilli et al., 2011**. Grilli, S. T., Harris, J. C., & Tajalli Bakhsh, T. (2011). Literature review of tsunami sources affecting tsunami hazard along the U. S. East Coast. Center for Applied Coastal Research, University of Delaware.

2.6.4-8 **Grilli et al., 2013a**. Grilli A.R. and S.T. Grilli. (2013a). Modeling of tsunami generation, propagation and regional impact along the upper U.S east coast from the Puerto Rico Trench. *Research Report no.* CACR-13-02. NTHMP Award, #NA10NWS4670010, National Weather Service Program Office, 18 pps.

2.6.4-9 **Grilli et al., 2013b**. Grilli A.R. and S.T. Grilli (2013b). Modeling of tsunami generation, propagation and regional impact along the U.S. East Coast from the Azores Convergence Zone. *Research Report no.* CACR-13-04. NTHMP Award, #NA10NWS4670010, National Weather Service Program Office, 20 pps.

2.6.4-10 **Grilli et al., 2013c**. Grilli A.R. and S.T. Grilli. (2013c). Far-Field tsunami impact on the U.S. East Coast from an extreme flank collapse of the Cumbre Vieja Volcano (Canary Island). *Research Report no.* CACR-13-03. NTHMP Award, #NA10NWS4670010, National Weather Service Program Office, 13 pps.

2.6.4-11 **Grilli et al., 2013d**. Grilli, S.T., C. O'Reilly and T. Tajalli-Bakhsh. (2013). Modeling of SMF tsunami generation and regional impact along the upper U.S. East Coast. *Research Report no.* CACR-13-05. NTHMP Award, #NA10NWS4670010, National Weather Service Program Office, 46 pps.

2.6.4-12 **Kirby et al., 2013**. Kirby, J.T., Shi, F., Tehranirad, B., Harris, J.C. and Grilli, S.T. (2013). Dispersive tsunami waves in the ocean: Model equations and sensitivity to dispersion and Coriolis effects. Ocean Modeling, 62, 39-55, doi:10.1016/j.ocemod.2012.11.009.

2.6.4-13 **Locat et al., 2009**. Locat J., H. Lee, U. ten Brink, D. Twichell, E. Geist, and M. Sansoucy. (2009). Geomorphology, stability, and mobility of the Currituck slide. Marine Geology, 264, 28-40.

2.6.4-14 **NOAA, 2012a**. NOAA National Geophysical Data Center (NGDC). (n.d.). NOAA/WDC Tsunami Runup. Retrieved November 8, 2012, from NOAA National Geophysical Data Center (NGDC). http://www.ngdc.noaa.gov/hazard/tsu_db.shtml.

2.6.4-15 **NOAA, 2012b**. NOAA Coastal Services Center (CSC), 2012 USACE Post Hurricane Sandy Topographic LiDAR: Central Connecticut, http://www.csc.noaa.gov/dataviewer/#

2.6.4-16 **NOAA, 2013a**. Tides and Currents: Watch Hill, RI Tide Offset, Watch Hill, RI, Station 8458694. Retrieved 28 February 2014, Last Modified 15 October 2013. http://tidesandcurrents.noaa.gov/noaatidepredictions/NOAATidesFacade.jsp?Stationid=8458694

2.6.4-17 **NOAA, 2013b**. Tides and Currents: Tide and Water Level Data: Verified Data, Newport, RI, Station 8452660. Retrieved 19 February 2013, Available at: http://tidesandcurrents.noaa.gov/waterlevels.html?id=8452660

2.6.4-18 **NOAA, 2013c**. Tides and Currents: Montauk, NY Updated Mean Sea Level Trends, Montauk, NY, Station 8510560. Retrieved 11 March 2014, Last Modified 15 October 2013. Available at: http://tidesandcurrents.noaa.gov/sltrends/sltrends_update.shtml?stnid=8510560

2.6.4-19 **NRC, 2011**. "Design Basis Flood Estimation for Site Characterization at Nuclear Power Plants - NUREG/CR-7046", U.S. Nuclear Regulatory Commission, November 2011. (ADAMS Accession No. ML11321A195).

2.6.4-20 **Okada, 1985**. Okada, Y Surface deformation due to shear and tensile faults in a half-space. B. Seismol. Soc. Am. 75(4): 1135-1154.

2.6.4-21 **Shi et al., 2012**. Shi, F., J.T. Kirby, J.C. Harris, J.D. Geiman and S.T. Grilli. (2012). A High-Order Adaptive Time-Stepping TVD Solver for Boussinesq Modeling of Breaking Waves and Coastal Inundation. Ocean Modeling, 43-44, 36-5.

2.6.4-22 **ten Brink et al., 2008**. ten Brink, U. S., Twitchell, D., Geist, E., Chaytor, J., Locat, J., Lee, H., Buczkowski, B., Barkan, R., Solow, A., Andrews, B., Parsons, T., Lynett, P., Lin, J., and Sansoucy, M. (2008). Evaluation of tsunami sources with the potential to impact the U.S. Atlantic and Gulf Coasts. Report to the Nuclear Regulatory Commission. USGS. 322 pp.

Table 2.6-1: Parameters of Atlantic Ocean basin model grids used for the far-field source definition and initial propagation modeling with FUNWAVE-TVD

Source	Min. Longitude East (Degrees)	Max. Longitude East (Degrees)	Min. Latitude North (Degrees)	Max. Latitude North (Degrees)	Resolution	Spherical /Cartesian
CVV 450 km^3	-82	-5	10	45	1 arc-minute	Spherical
Lisbon M9	-82	-5	10	45	1 arc-minute	Spherical
PRT M9	-82	-50	10	45	1 arc-minute	Spherical

Table 2.6-2: Parameters of the SMF located offshore from the entrance to Long Island Sound (from Grilli et al., 2013d)

SMF Parameters		Description
T (m)	750	Maximum thickness
b (km)	30	Maximum down-slope length
w (km)	20	Maximum width
slope (deg.)	4	Local mean slope (deg.)
Location	(39.76N, 71.49W)	Coordinates of initial SMF location
θ (deg. N)	153	Direction of SMF motion
s_f (km)	15.8	Length of runout
t_f (seconds)	710	Time of motion
ε	0.717	Gaussian shape parameter

Table 2.6-3: Location and depth (relative to 3.23 feet NAVD88) of four stations defined in the 10m near-field local grids to compute time series of tsunami elevation

Stations	Longitude East (Degrees)	Latitude North (Degrees)	Depth (m)
1	-72.1764	41.3136	6
2	-72.1748	41.3066	9
3	-72.1648	41.2993	13
4	-72.1624	41.2839	15

Table 2.6-4: Grid dimensions and boundary conditions stations for local model grids used for the far-field source modeling with FUNWAVE-TVD

Local Grids	Number of Stations used as Boundary Conditions					Scale Factor	Grid size (Nx*Ny)
	Total	East	West	South	North		
1: 600 m	648	260	0	288	0	3	1162*778
2:150 m	310	108	0	202	0	4	805*429
3: 40 m	519	159	159	201	0	4	801*633
4: 10 m	443	145	145	153	0	4	609*577

Table 2.6-5: Grid dimensions and boundary conditions stations for local model grids used for the near-field source modeling with FUNWAVE-TVD

Local Grids	Number of Stations used as Boundary Conditions					Scale Factor	Grid size (Nx*Ny)
	Total	East	West	South	North		
1: 500 m	Grid initialized with NHWAVE Source						1500*1300
2: 120 m	1318	517	0	801	0	4	1000*517
3: 30 m	754	174	174	203	0	4	1009*909
4: 10 m	537	170	170	197	0	3	589*508

Table 2.6-6: Summary Table of Tsunamigenic Events

Tsunami Source	Maximum Water Surface Elevation on the Western side of the site (feet MSL)	Maximum Water Surface Elevation at MPS2 and MPS3 (feet MSL)	Maximum Water Surface Elevation on the Eastern Side of the Site (feet MSL)	Maximum Depth of Water Above MPS2 Average Site Grade (14 ft MSL)	Depth of Water Above MPS3 Average Site Grade (24 ft MSL)	Time from Source Event to Tsunami Reaching MPS (hr)
PRT	14.7	8.6	9.8	0	0	5.4
Lisbon	--	--	4.6	0	0	7.5
CVV	21.1	14.7	12.0	0.7	0	8.7
SMF	15.1	10.3	10.6	0	0	2.3

Figure 2.6-1: Site Location and NOAA Tidal Stations

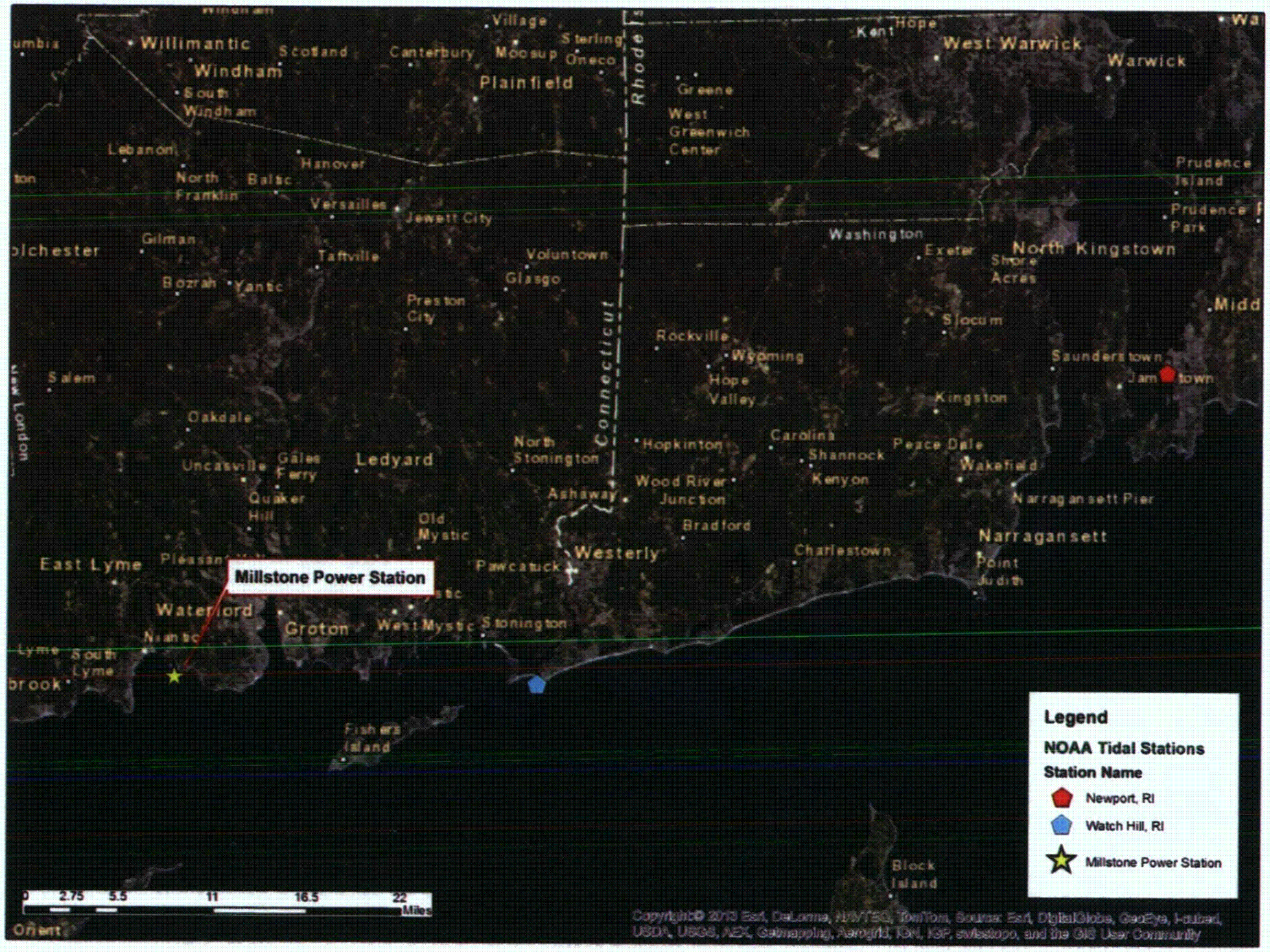

Figure 2.6-2: Location (bathymetry (< 0) and topography (> 0) as color scale in meters) for an extreme Lisbon M9 co-seismic source

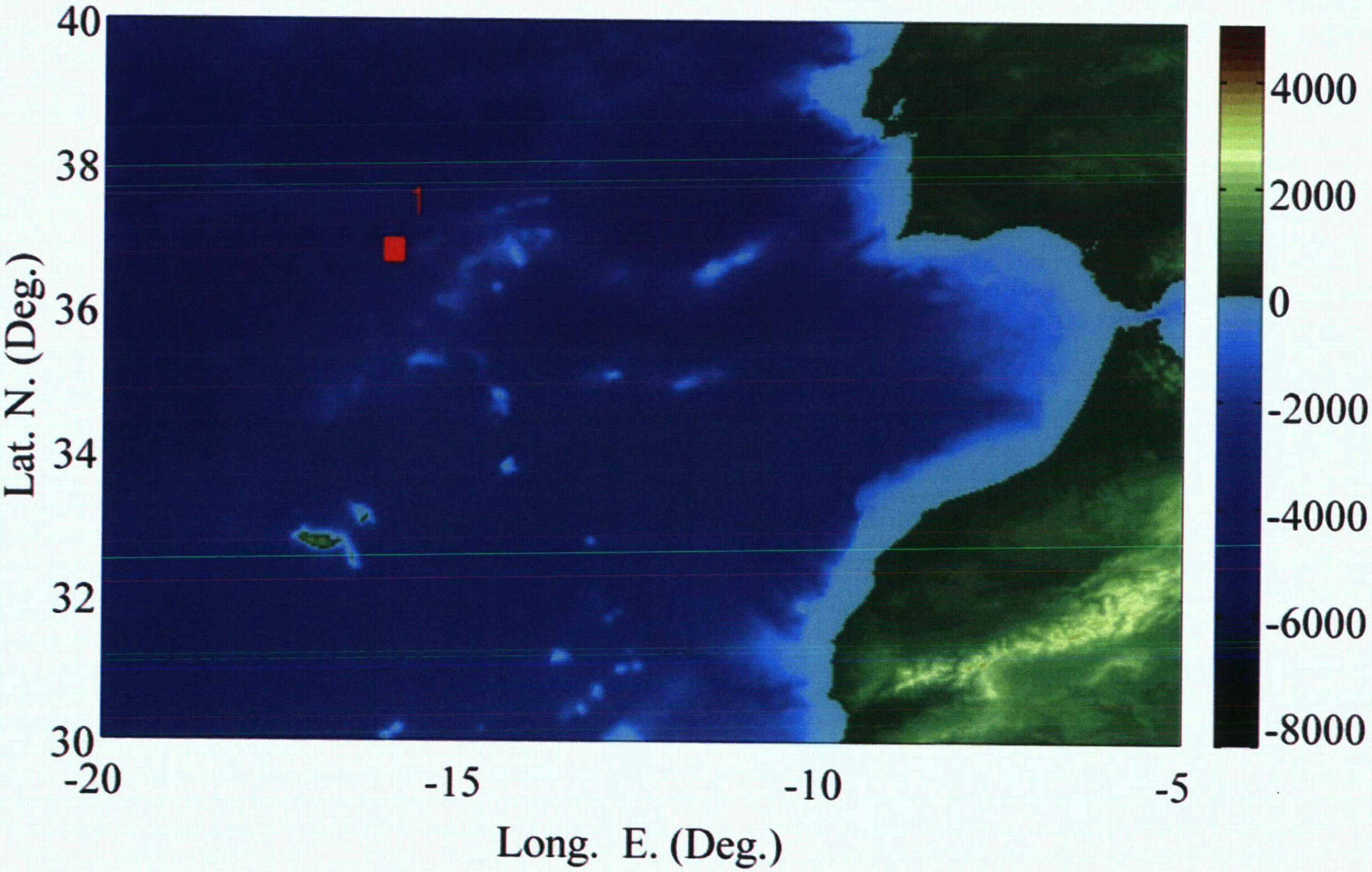

Figure 2.6-3: Far-field Atlantic Ocean basin grids used in simulations of the: CVV 450 km^3 subaerial landslide (red triangle symbol), Lisbon M9 co-seismic (red square symbol). Color scale indicates depth (<0) and topography (>0) in meters from the ETOPO-1 database.

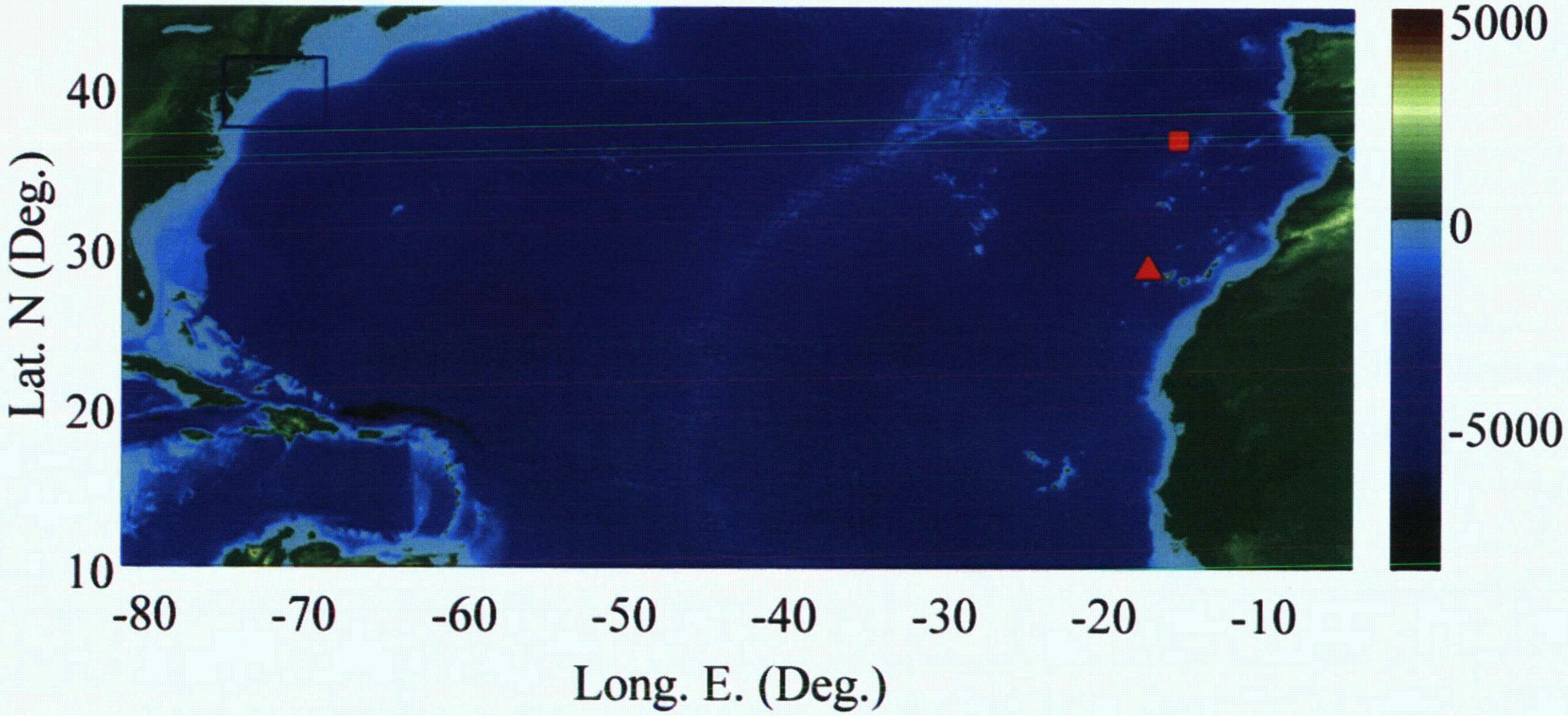

Figure 2.6-4: Currituck SMF proxy source bathymetry and elevation over the area of the 500 m regional grid used in SMF modeling with NHWAVE and FUNWAVE-TVD. Bathymetry (depth is color scale in meters) and transect (black line) through Currituck SMF proxy in NTHMP Area 2 (Grilli et al., 2013d). The white dot represents the initial location of the SMF before motion.

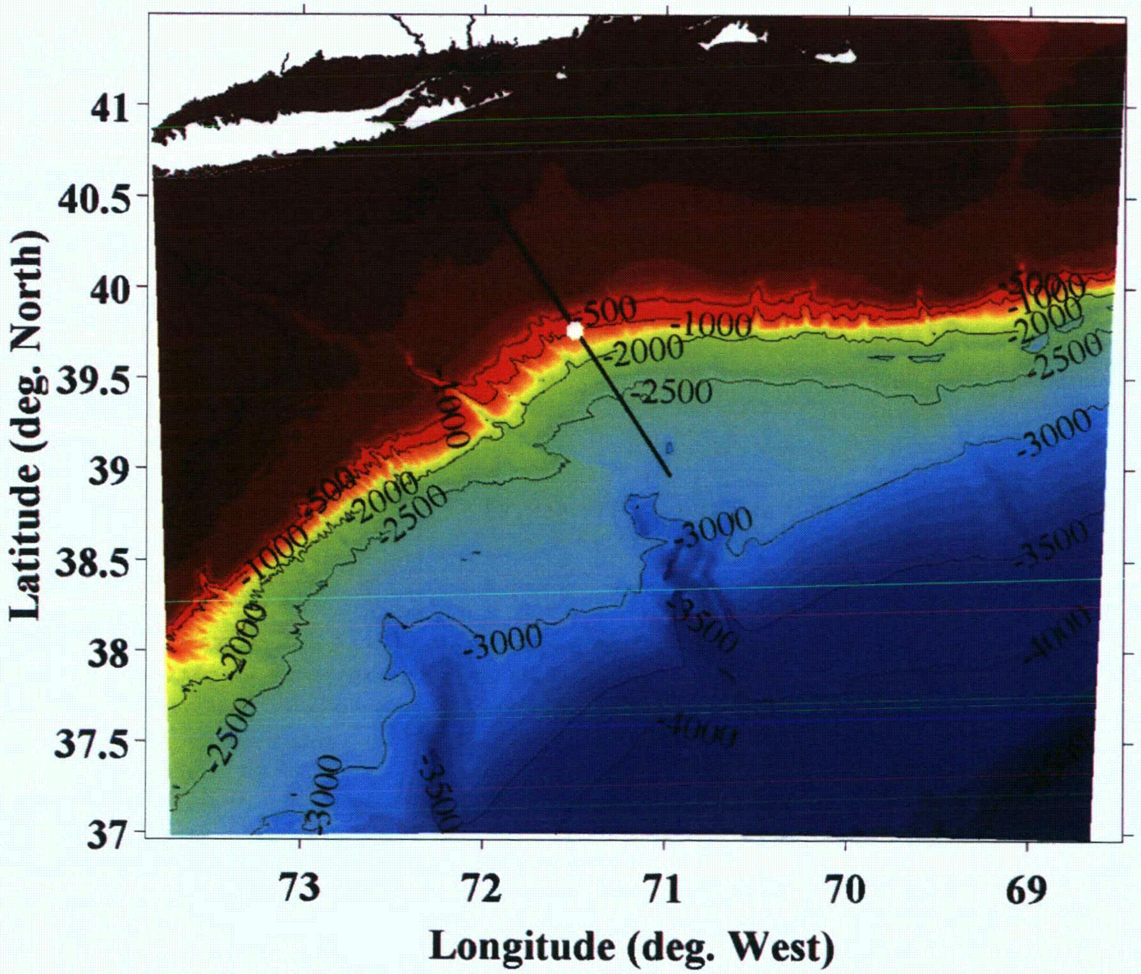

Figure 2.6-5: Location of four near shore stations used to extract tsunami time-series output

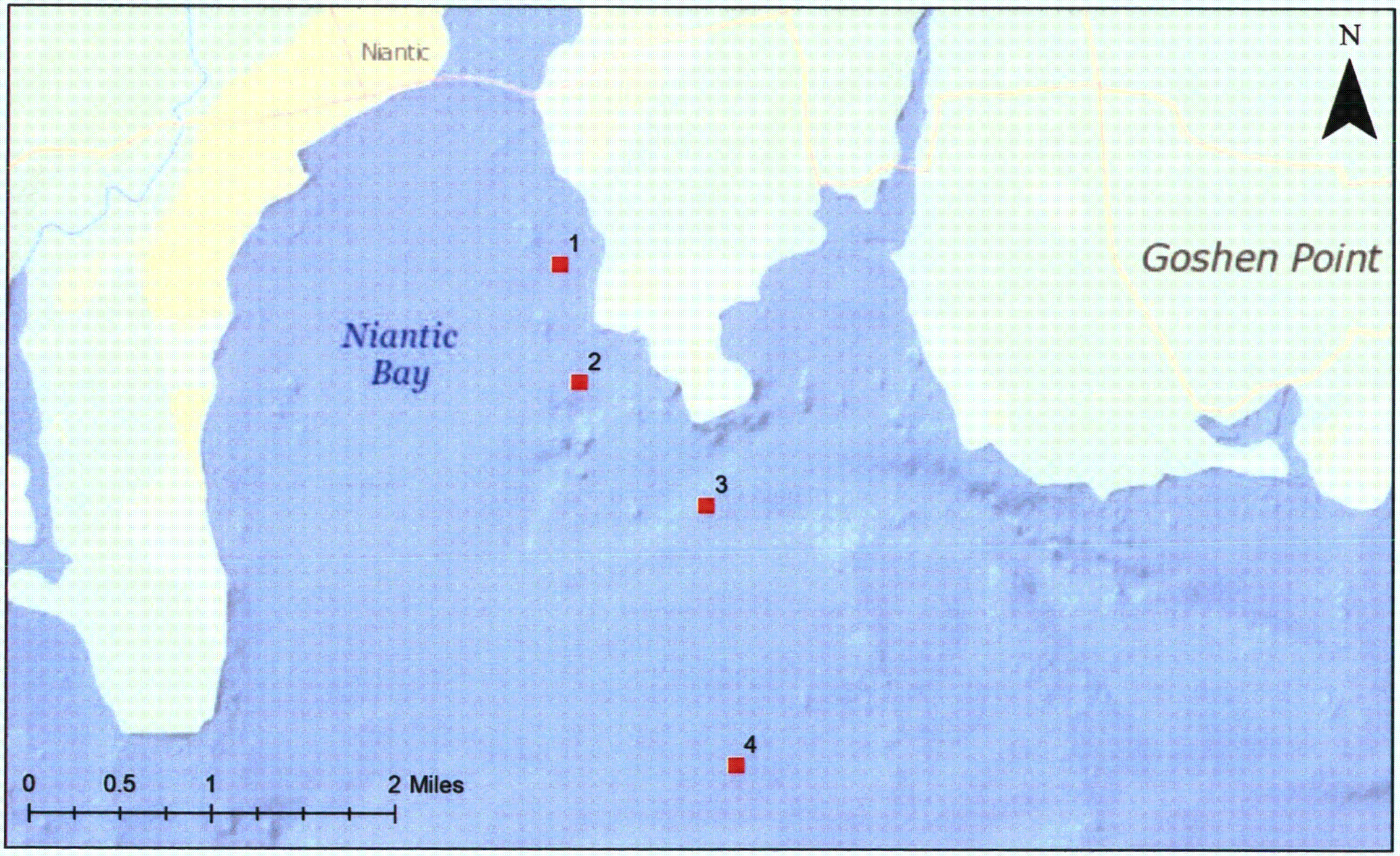

Figure 2.6-6: PRT M9 co-seismic source. (a-c) Tsunami surface elevation (color scale in meters) computed with FUNWAVE-TVD in the 1 degree spherical grid (Table 1), at 30, 102 and 200 minutes after the start of the PRT event. (d) Maximum computed surface elevation (color scale in meters NAVD88).

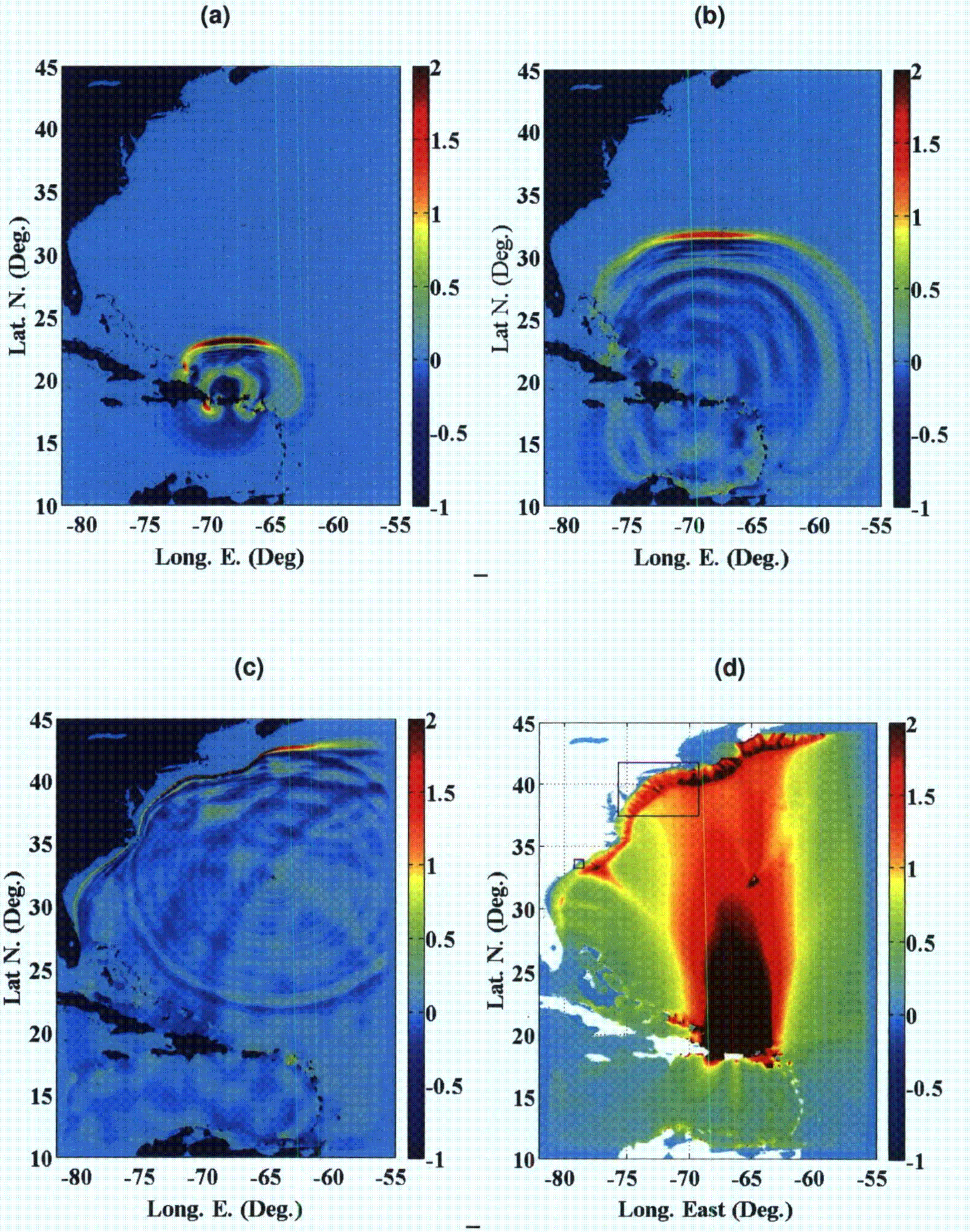

Figure 2.6-7: Initial surface elevation (color scale in meters) for an extreme PRT M9 co-seismic source

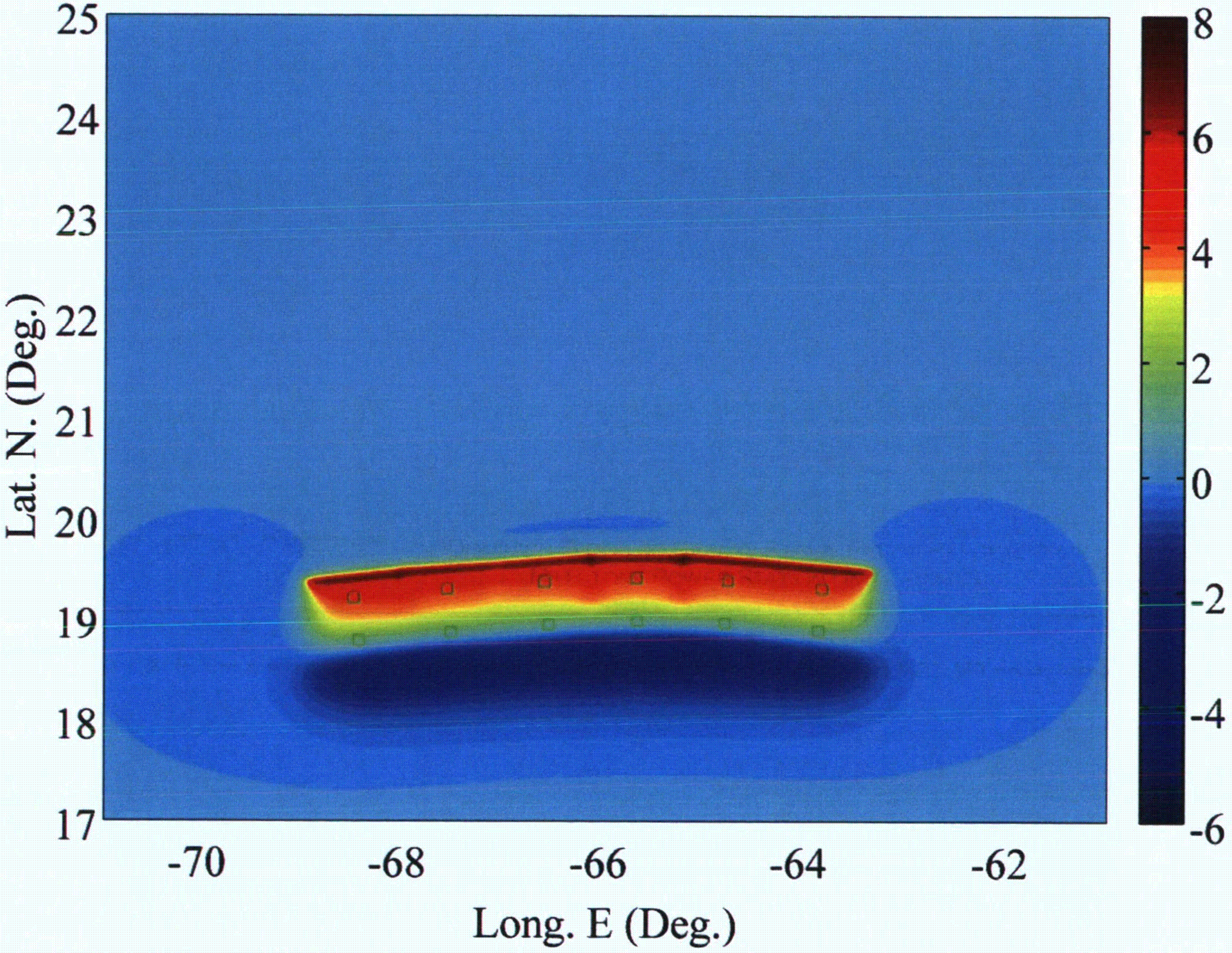

Figure 2.6-8: PRT M9 co-seismic source. Maximum water surface elevation (color scale in meters; referenced to 3.23 ft NAVD88) computed in the same grid as (b) based on topographic and bathymetric data from the Montauk DEM revised with post-Sandy LIDAR survey.

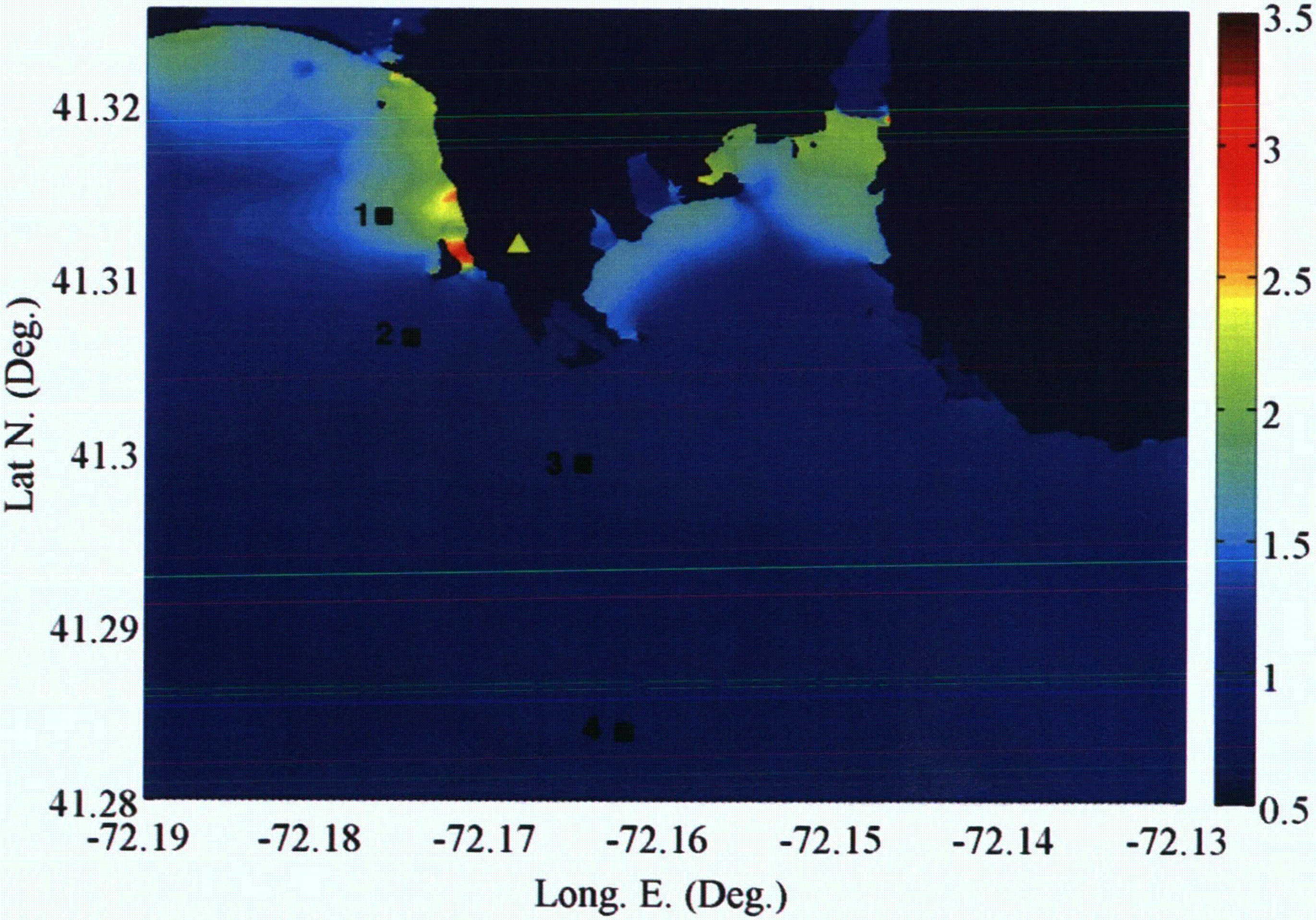

Figure 2.6-9: PRT M9 co-seismic source. Maximum water surface elevation (color scale in meters; referenced to 3.23 ft NAVD88) computed in the “10” meter near-field local grids, centered around the MPS site (marked by a yellow triangle) based the Montauk DEM.

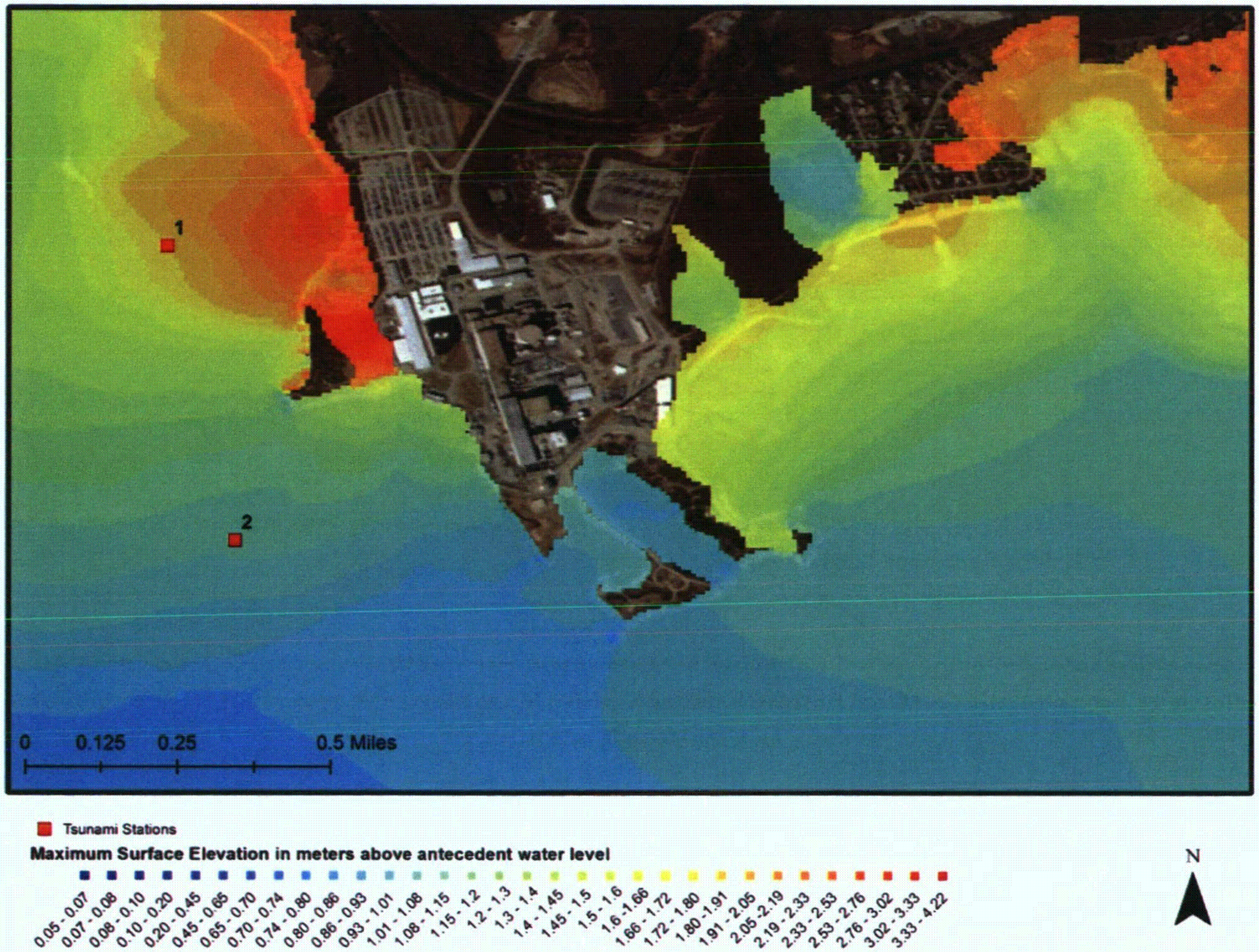

Figure 2.6-10: Initial surface elevation (color scale in meters) for an extreme Lisbon M9 co-seismic source

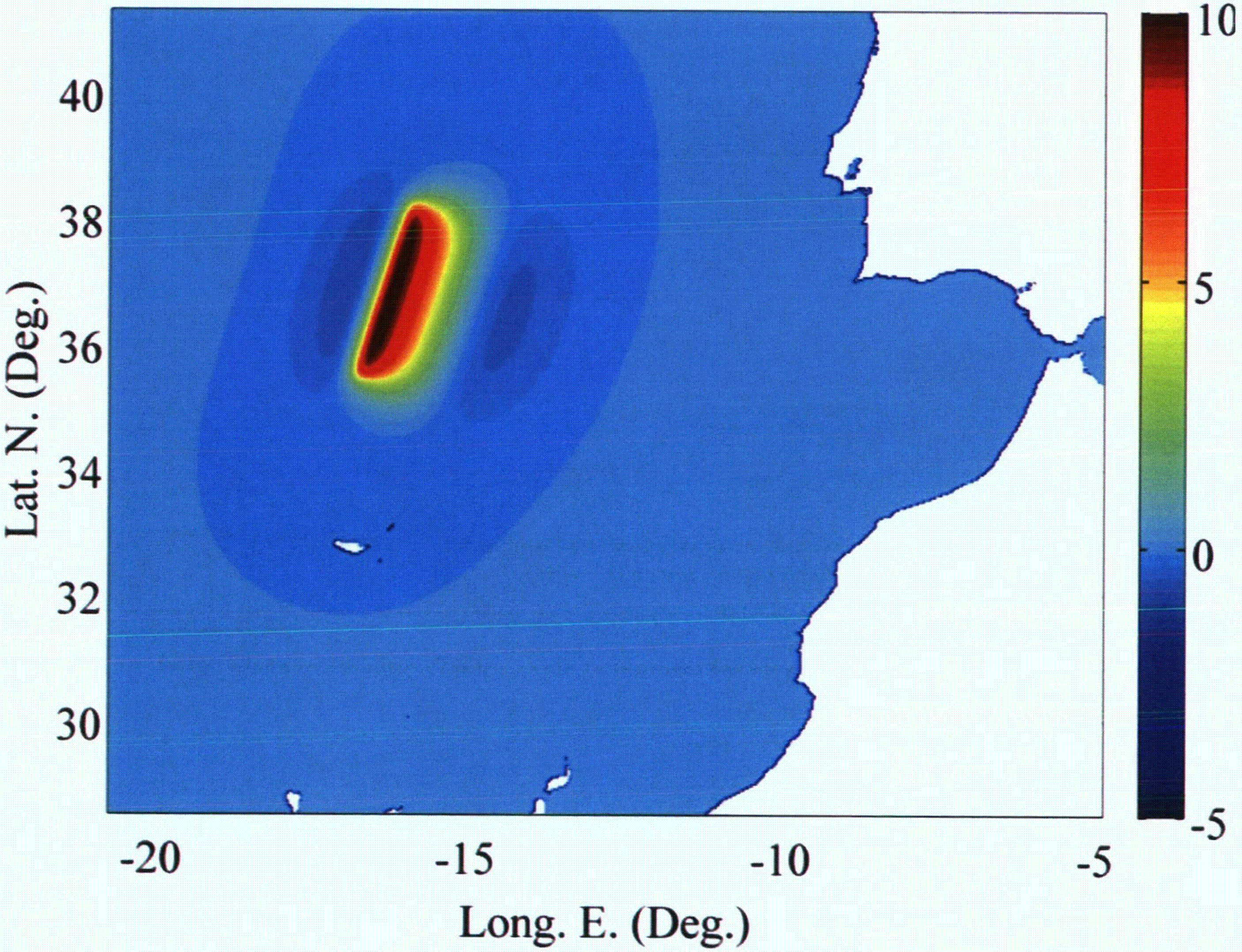

Figure 2.6-11: Lisbon M9 co-seismic source. Snapshots of tsunami surface elevation (color scale in meters) at 50, 120 and 510 min, after the event.

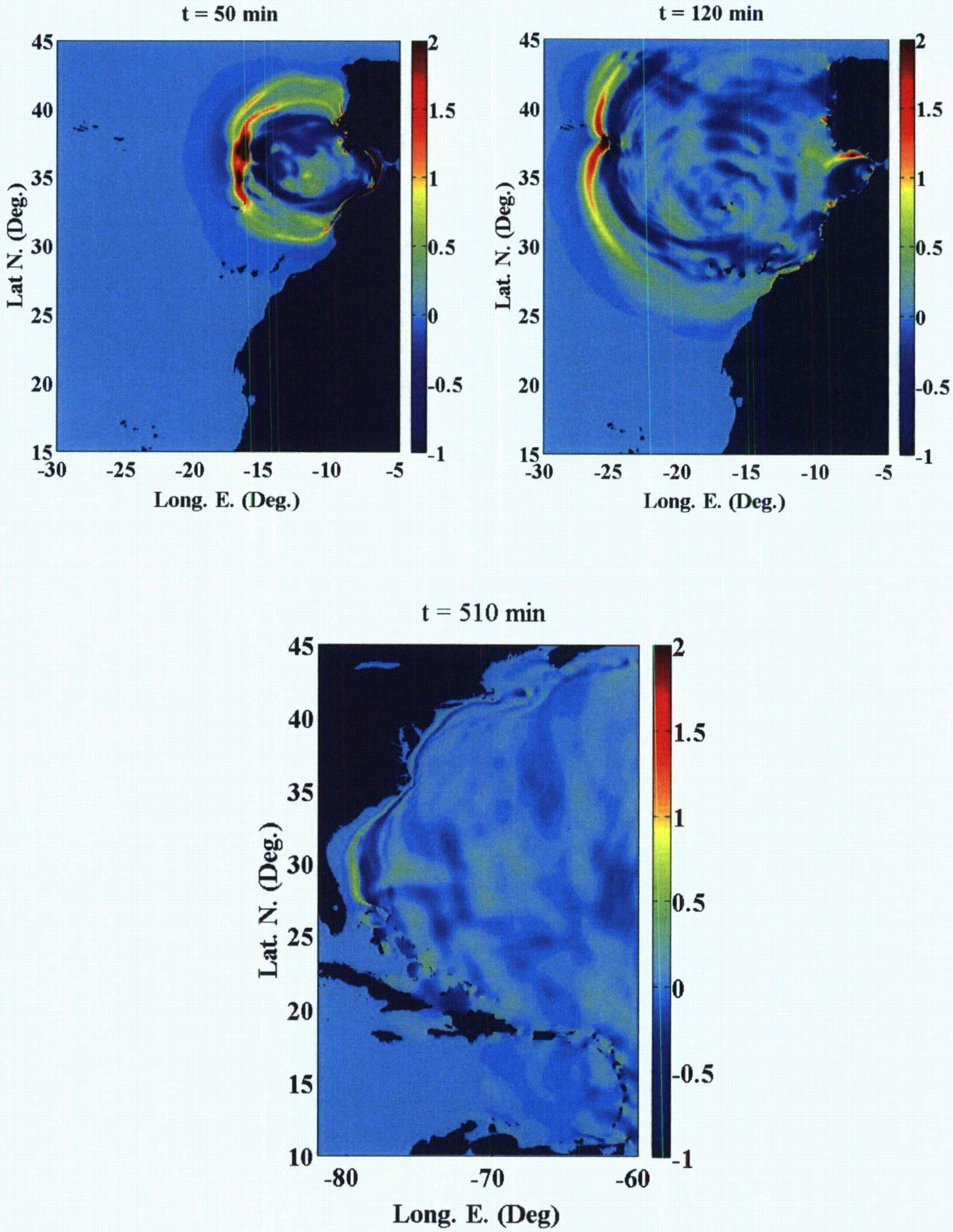

Figure 2.6-12: Lisbon M9 co-seismic source. Maximum water surface elevation (color scale in meters; referenced to 3.23 ft NAVD88) computed in the "10" meter near-field local grid centered around the MPS site (triangle).

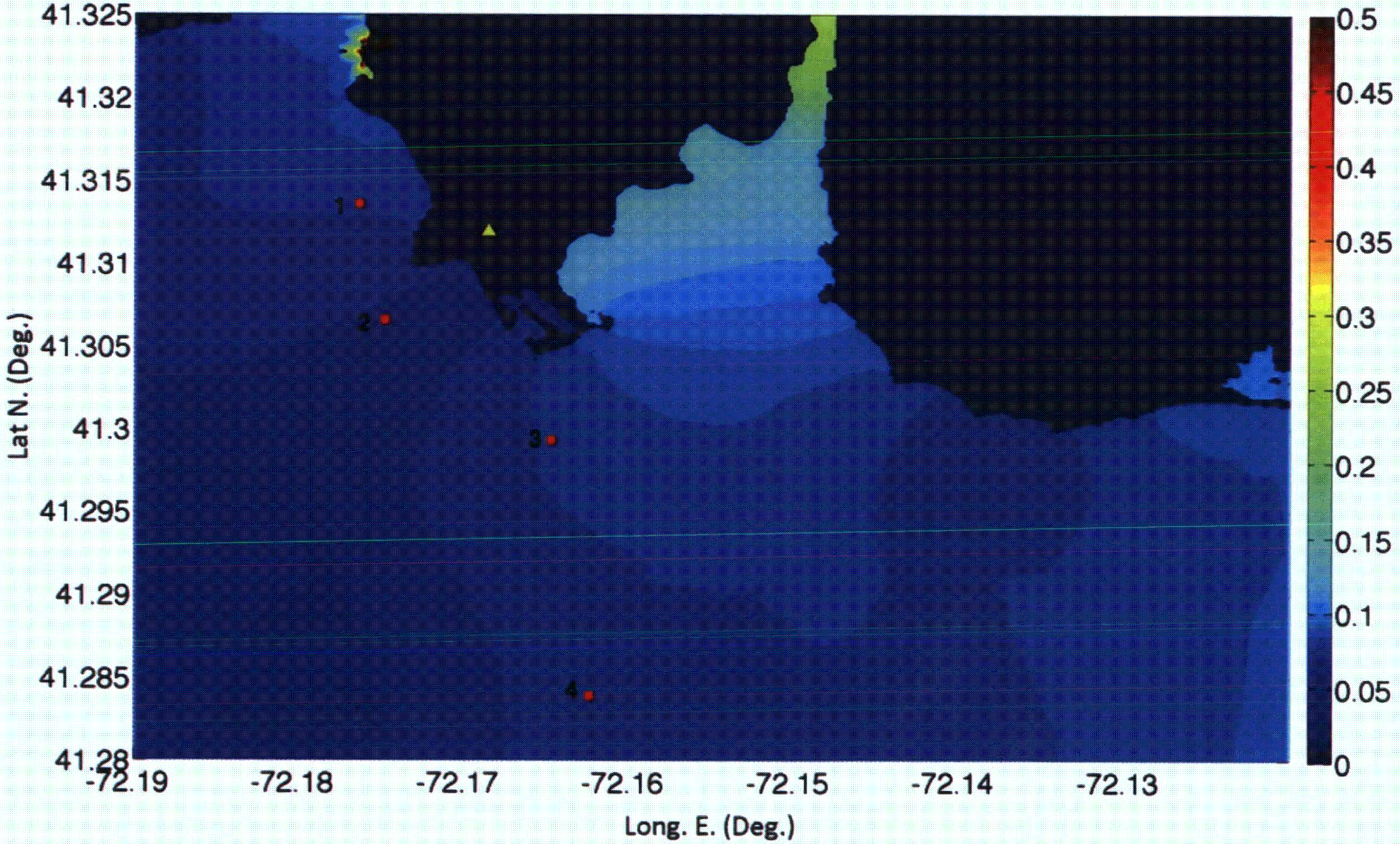

Figure 2.6-13: Lisbon M9 co-seismic source. Maximum water surface elevation (color scale in meters; referenced to 3.23 ft NAVD88) computed in the "10" meter near-field local grid centered around the MPS site.

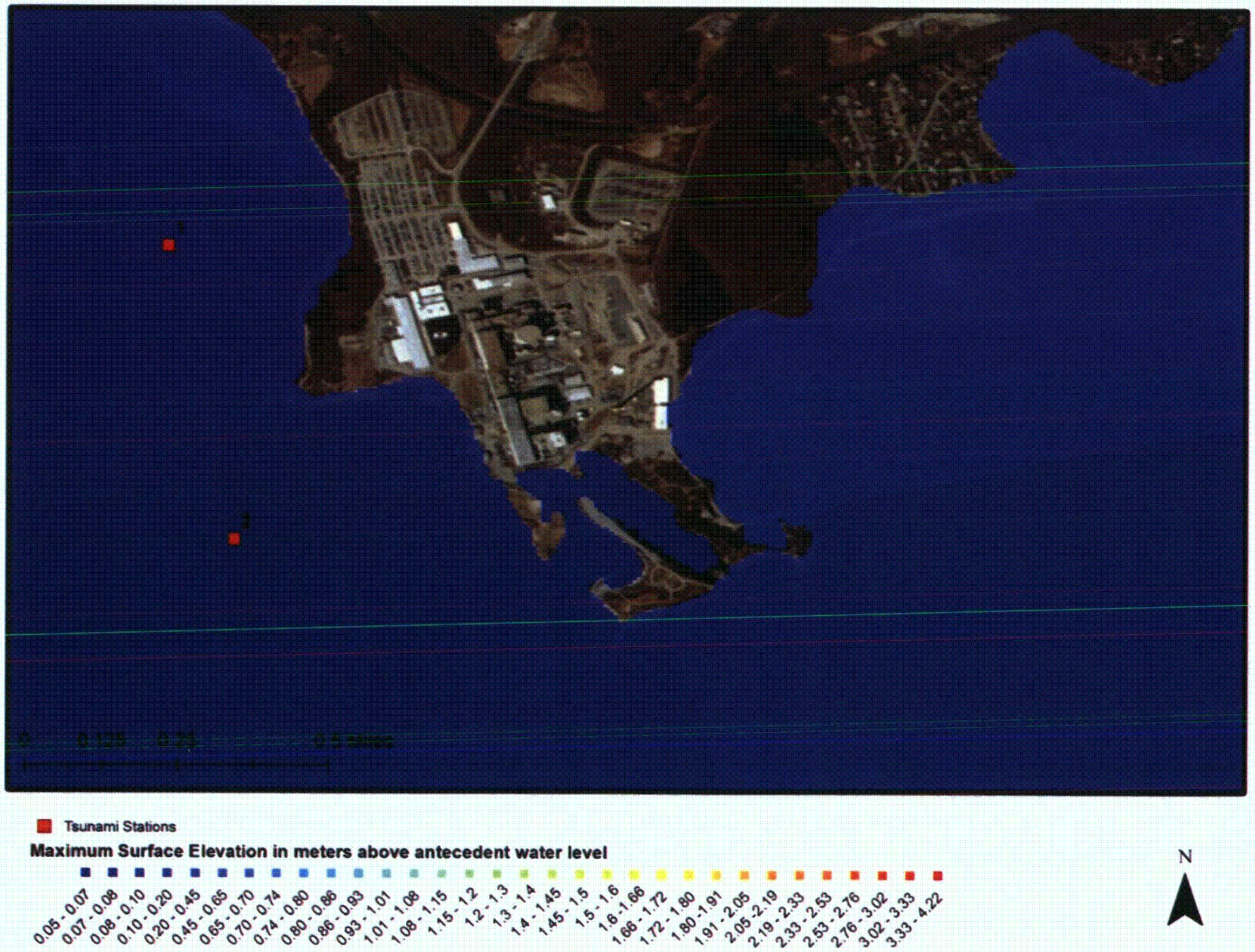

Figure 2.6-14: Lisbon M9 co-seismic source. Time series of surface elevation referenced to 3.23 ft NAVD88, computed in the "10" meter near-field local grid at 4 stations. Time is total time since the start of the PRT event.

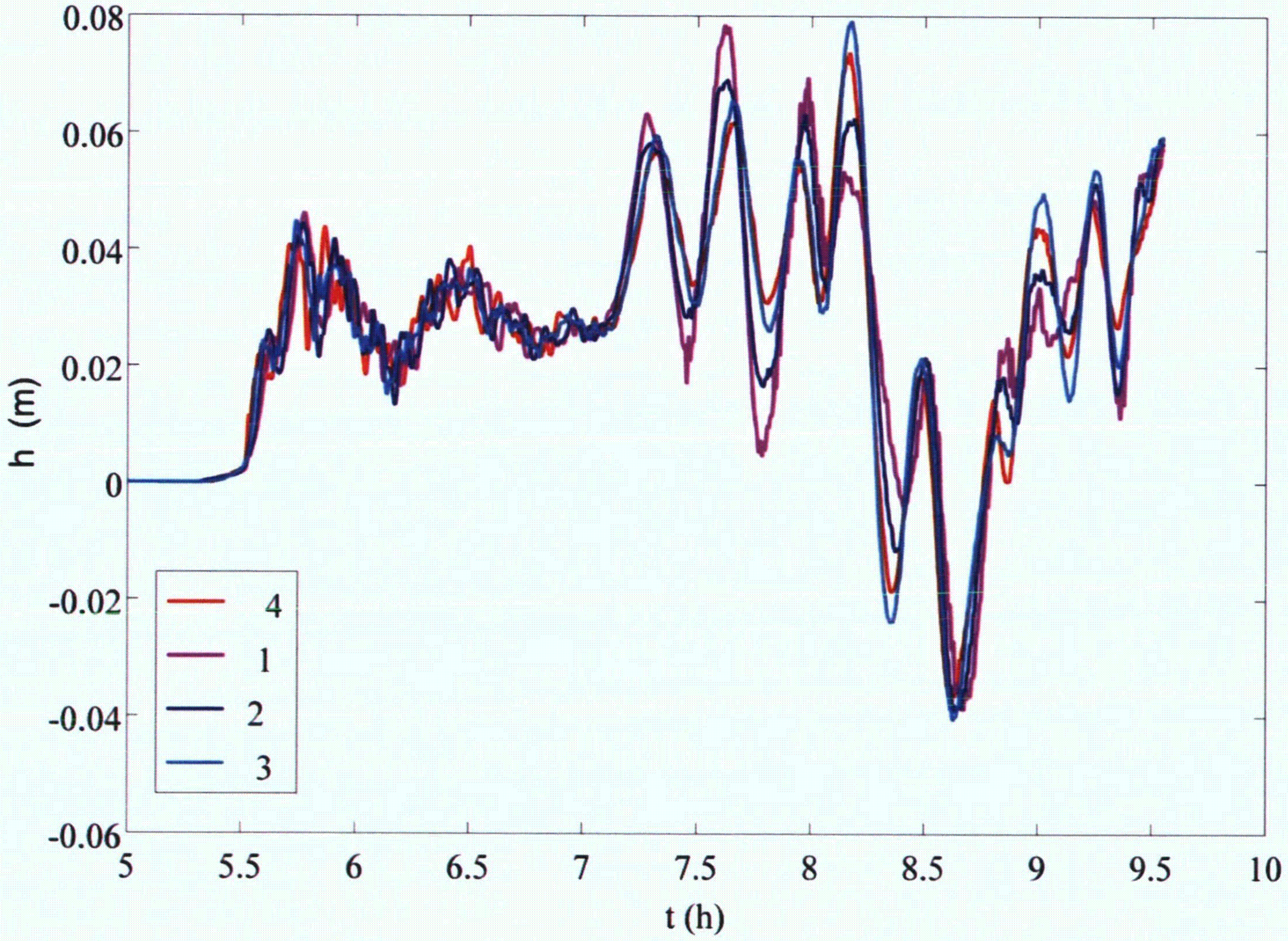

Figure 2.6-15: CVV 450 km^3 source. Left: Time series of tsunami surface elevation computed at stations (shown on right) versus time t after the start of the CVV event. Time axis is in hour after the tsunami source was defined in FUNWAVE-TVD (20 minutes after the CVV collapse). Right: Tsunami surface elevation (color scale in meter) computed with FUNWAVE-TVD in the 1 degree spherical grid, at 7h 20 min after the start of the CVV event.

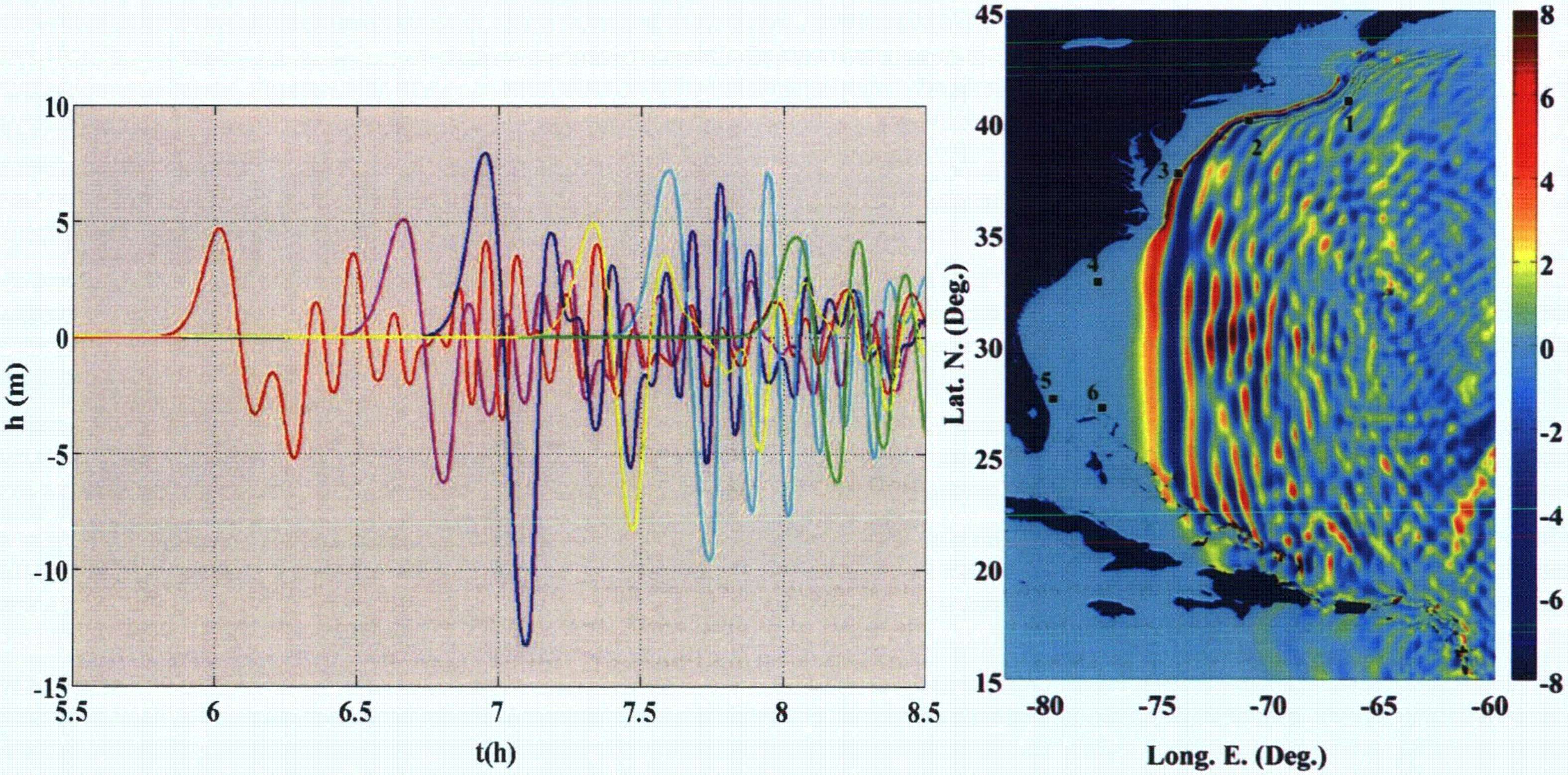

Figure 2.6-16: CVV 450 km^3 source. Maximum water surface elevation (color scale in meters; referenced to 3.23 ft NAVD88) computed in the "40" meter grid.

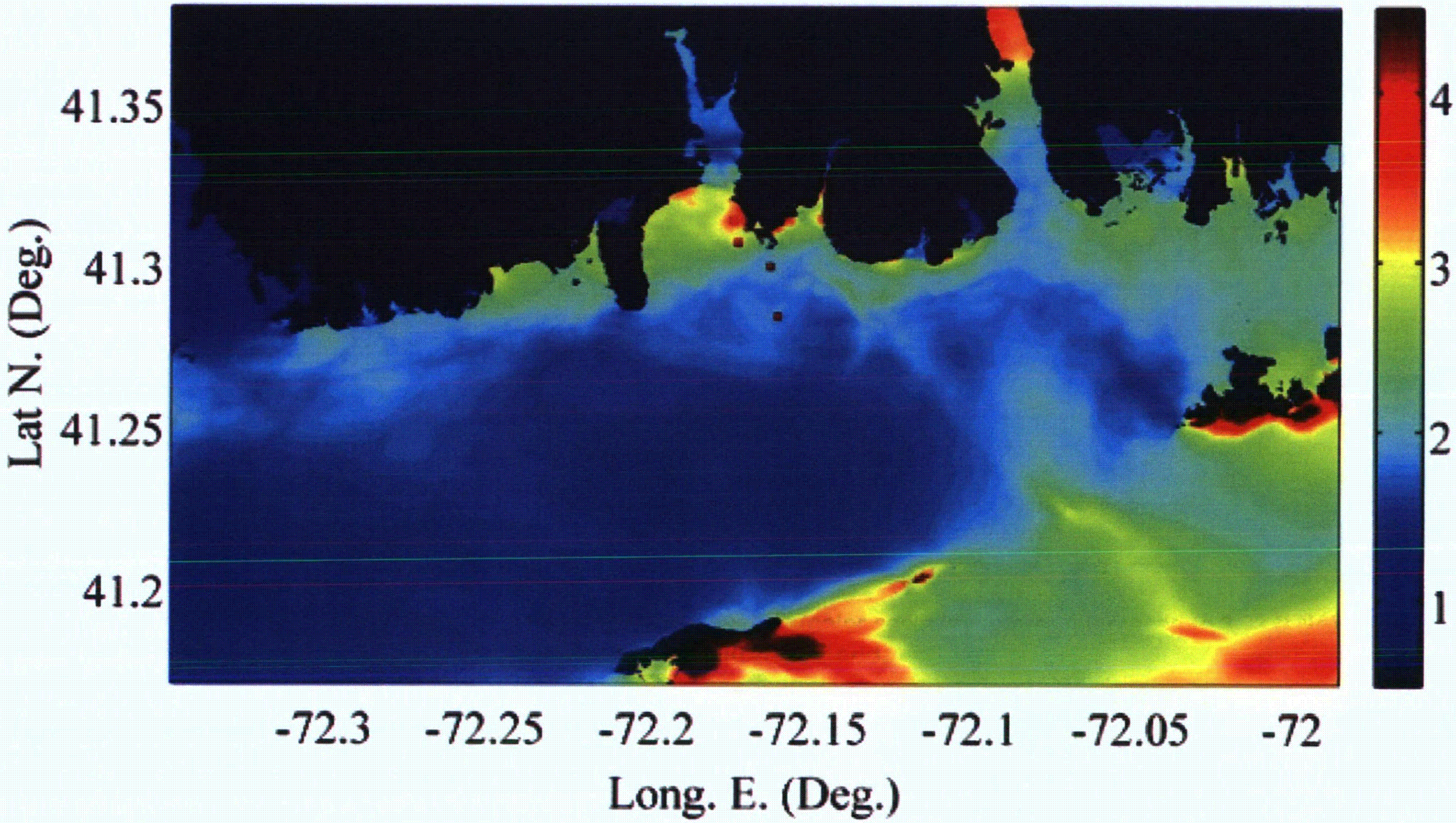

Figure 2.6-17: CVV 450 km^3 source. Maximum water surface elevation (color scale in meters; referenced to 3.23 ft NAVD88) computed in the "10" meter near-field local grids, centered around the MPS site (marked by a yellow triangle), based the Montauk DEM. Locations of stations 1-4 are also marked.

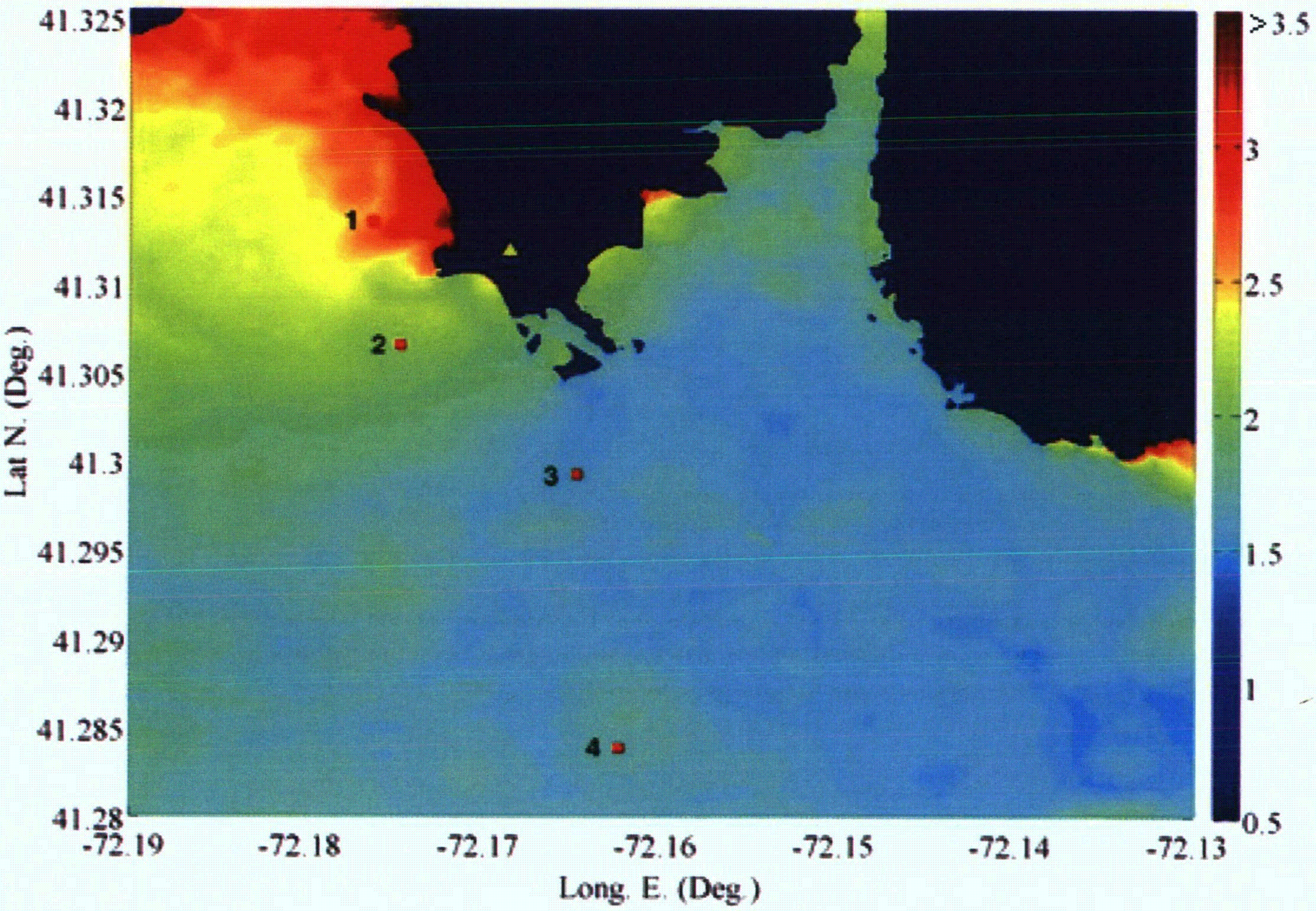

Figure 2.6-18: CVV 450 km^3 source. Maximum water surface elevation (color scale in meters; referenced to 3.23 ft NAVD88) computed in the "10" meter near-field local grids, centered around the MPS site (marked by a yellow triangle), based the Montauk DEM revised with the post-Sandy LIDAR survey. Locations of stations 1-4 are also marked.

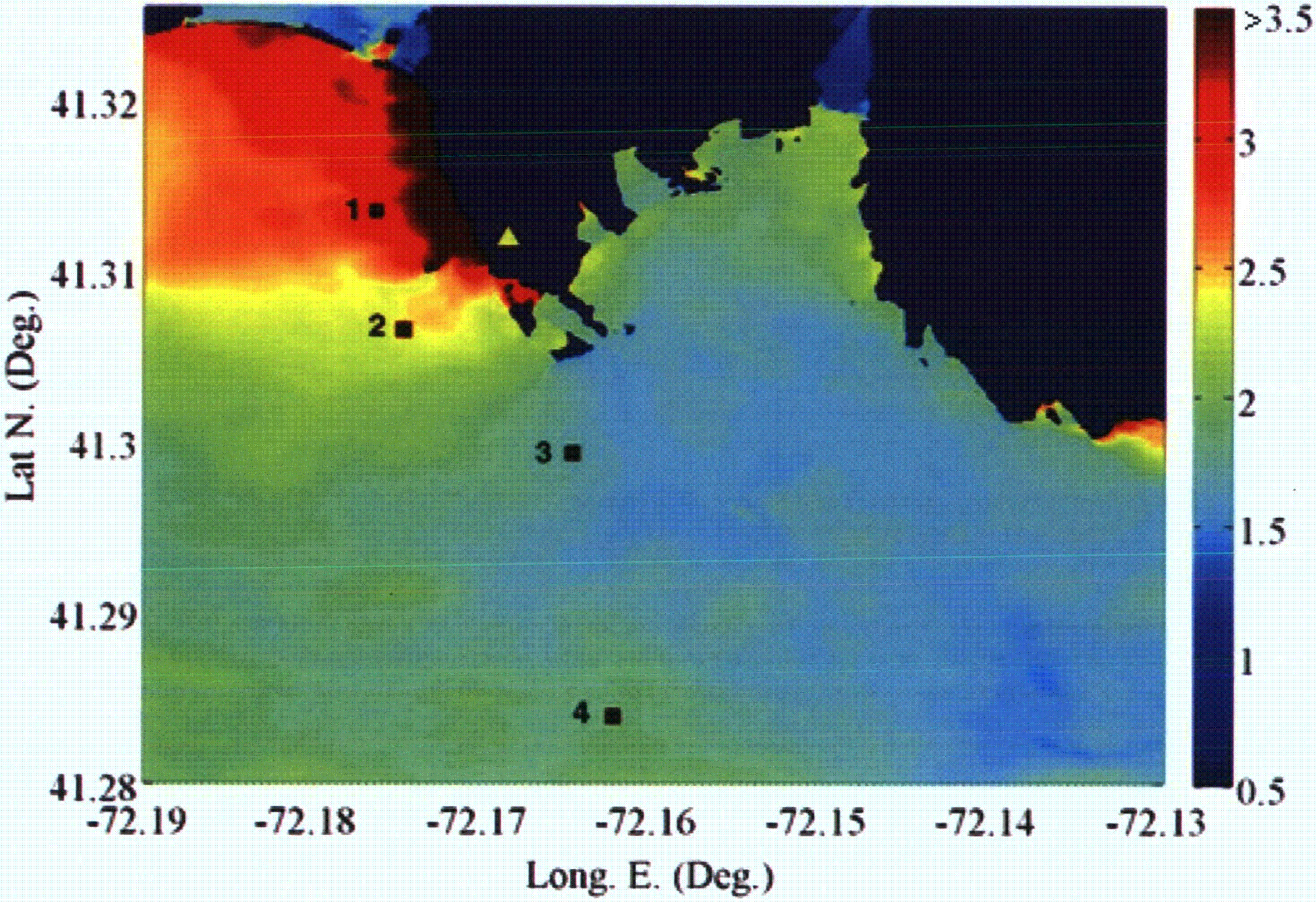

Figure 2.6-19: CVV 450 km^3 source. Locations of stations 1 and 2 are also marked.

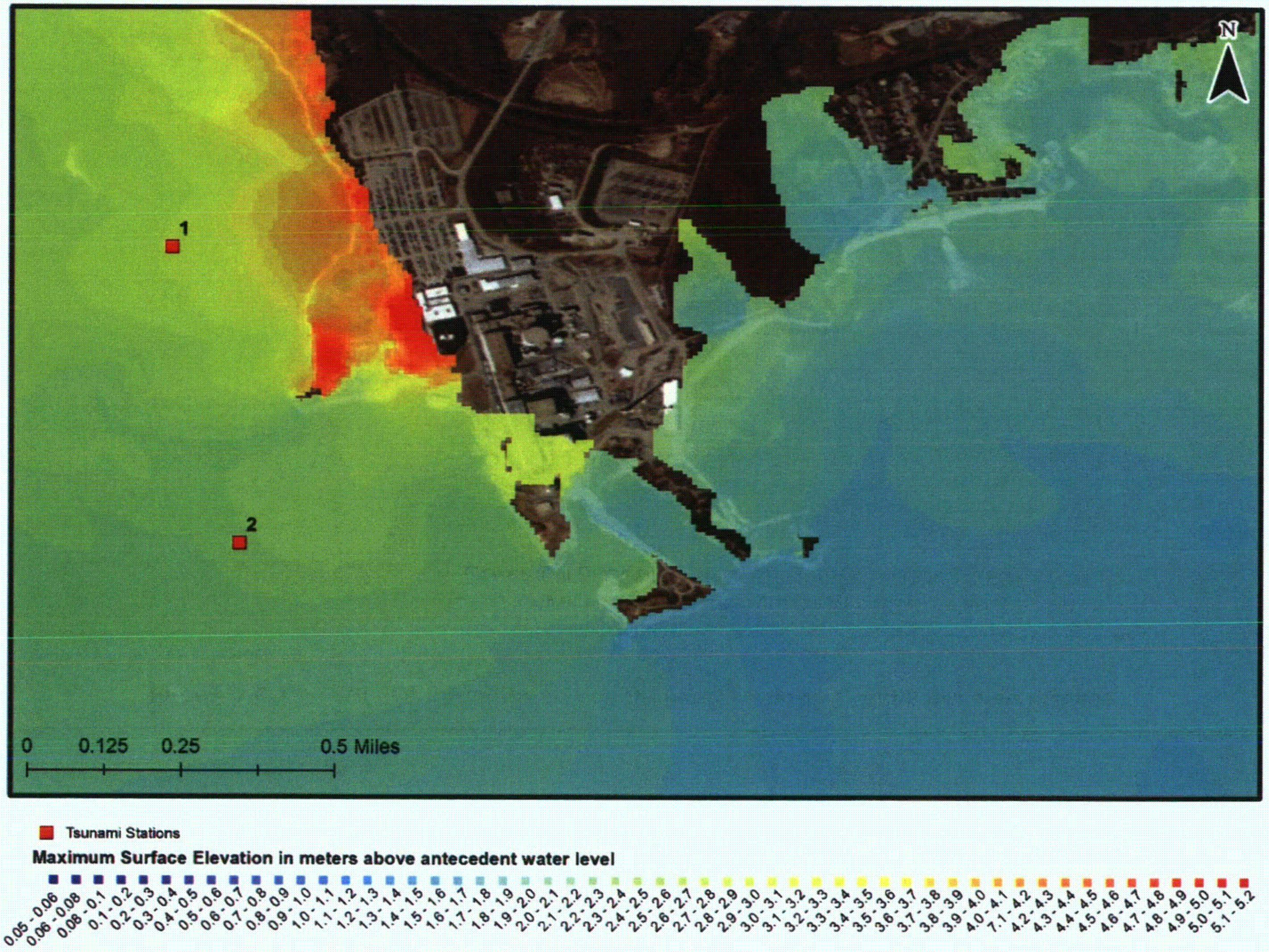

Figure 2.6-20: CVV 450 km^3 source. Time series of surface elevation referenced to 3.23 ft NAVD88, computed in the "10" meter near-field local grids, at 4 stations. Time is total time since the start of the CVV event. Topography and bathymetry based on the Montauk DEM (dash); Montauk DEM revised with post-Sandy LIDAR survey (solid).

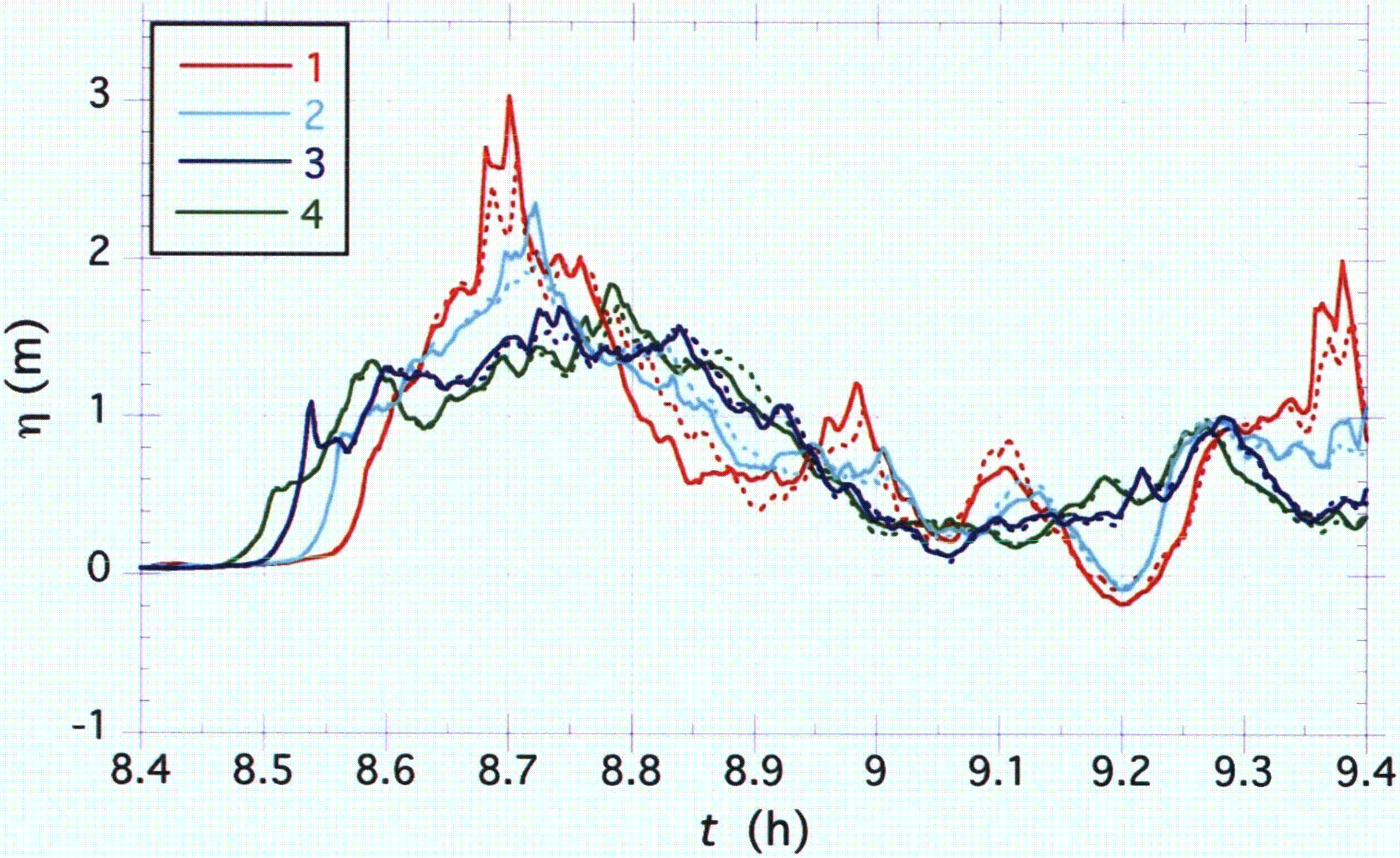

Figure 2.6-21: Initial surface elevation for SMF tsunami source (color scale in meters) computed with the 3D model NHWAVE based on SMF motion, after 13.3 minutes (with initial footprint marked by the black ellipse).

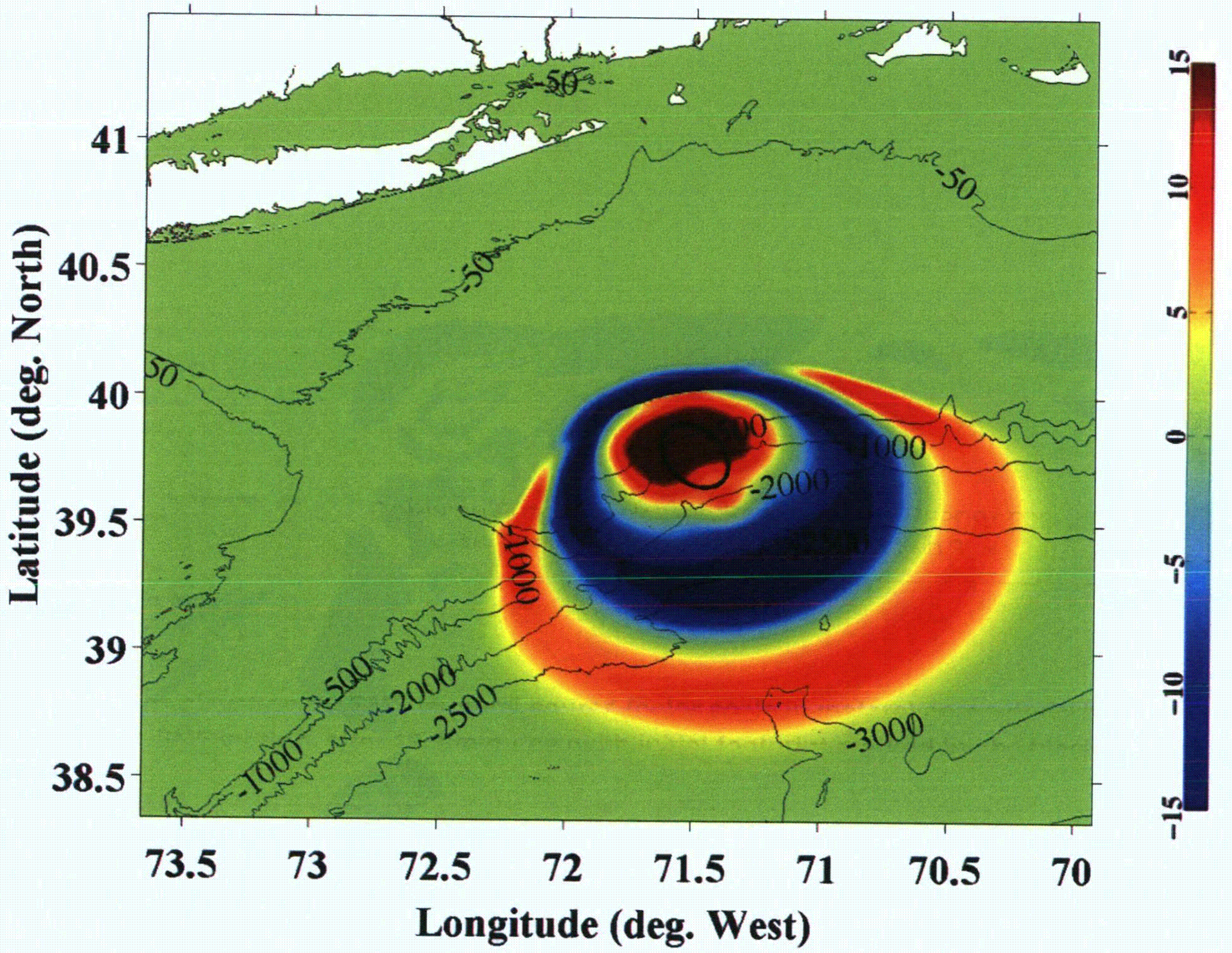

Figure 2.6-22: Currituck Proxy SMF source. Maximum water surface elevation (color scale in meters; referenced to 3.23 ft NAVD88) computed in the "30" meter grid.

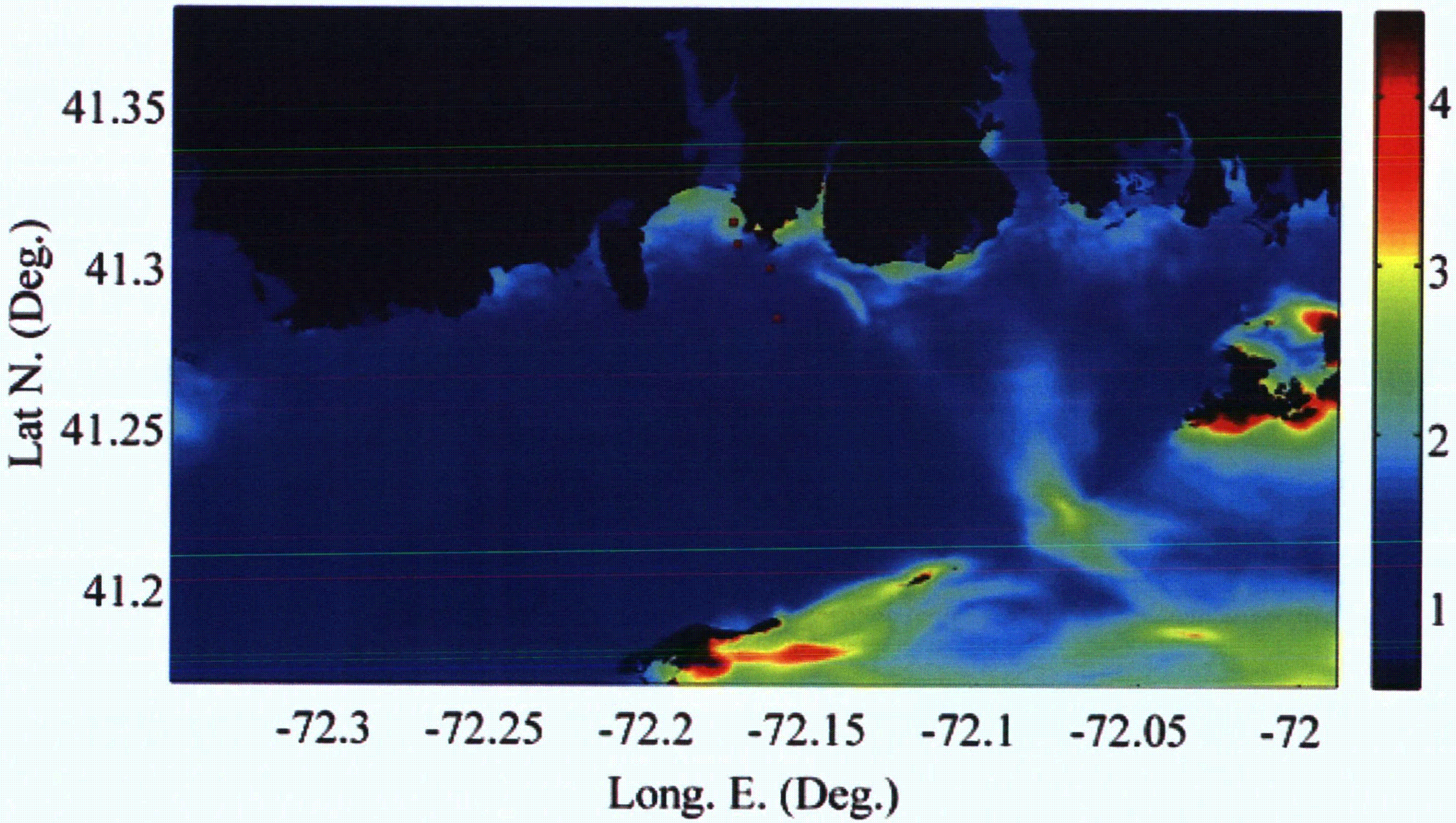

Figure 2.6-23: Currituck Proxy SMF source. Maximum water surface elevation (color scale in meters; referenced to 3.23 ft NAVD88) computed in the "10" meter near-field local grids, centered around the MPS site (marked by a yellow triangle), based on topographic and bathymetric data from the Montauk DEM revised with the post-Sandy LIDAR survey.

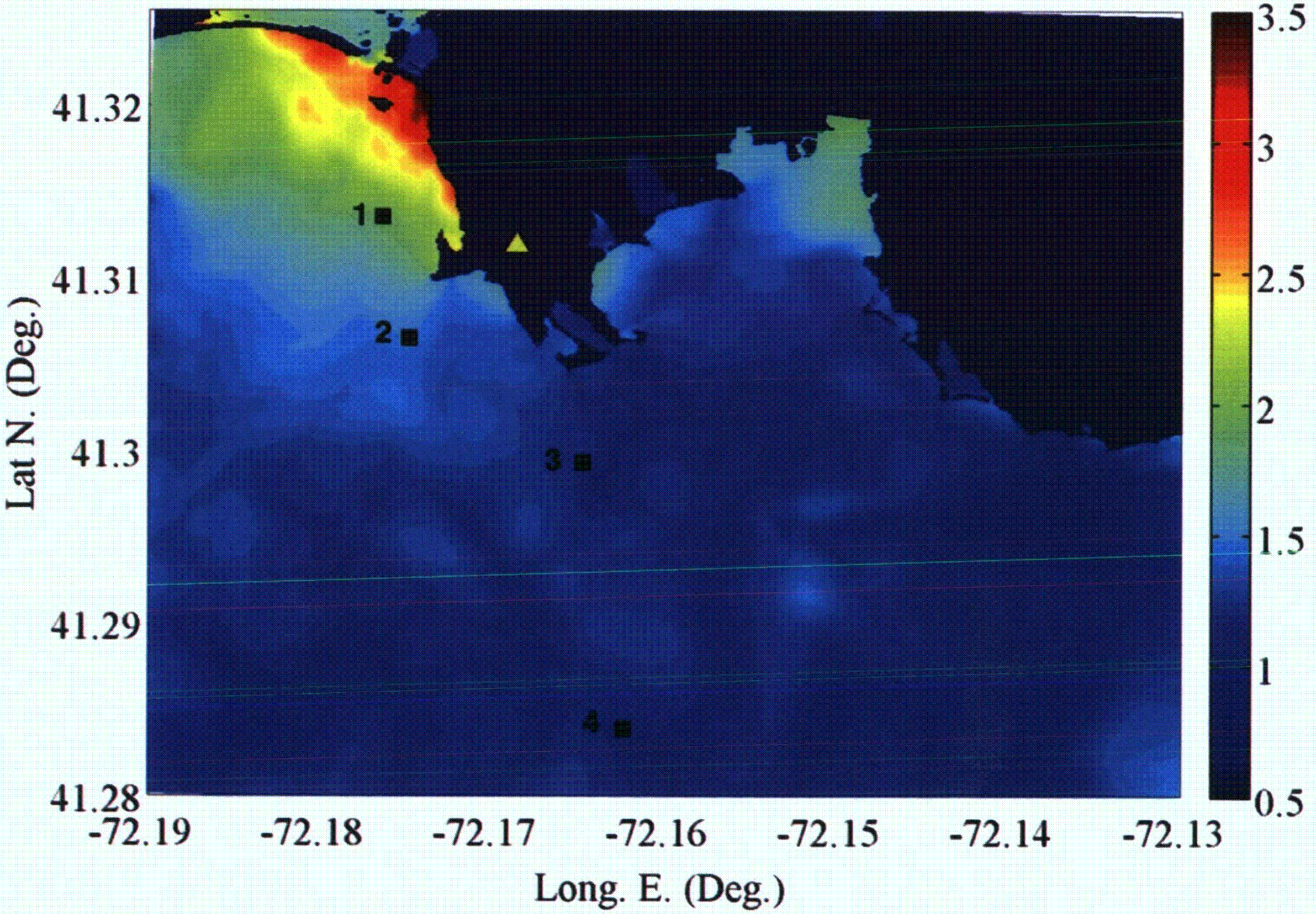

Figure 2.6-24: Currituck Proxy SMF source. Time series of surface elevation referred to 3.23 ft NAVD88, computed in the "10" meter near-field local grids. Time is total time since the start of the SMF event.

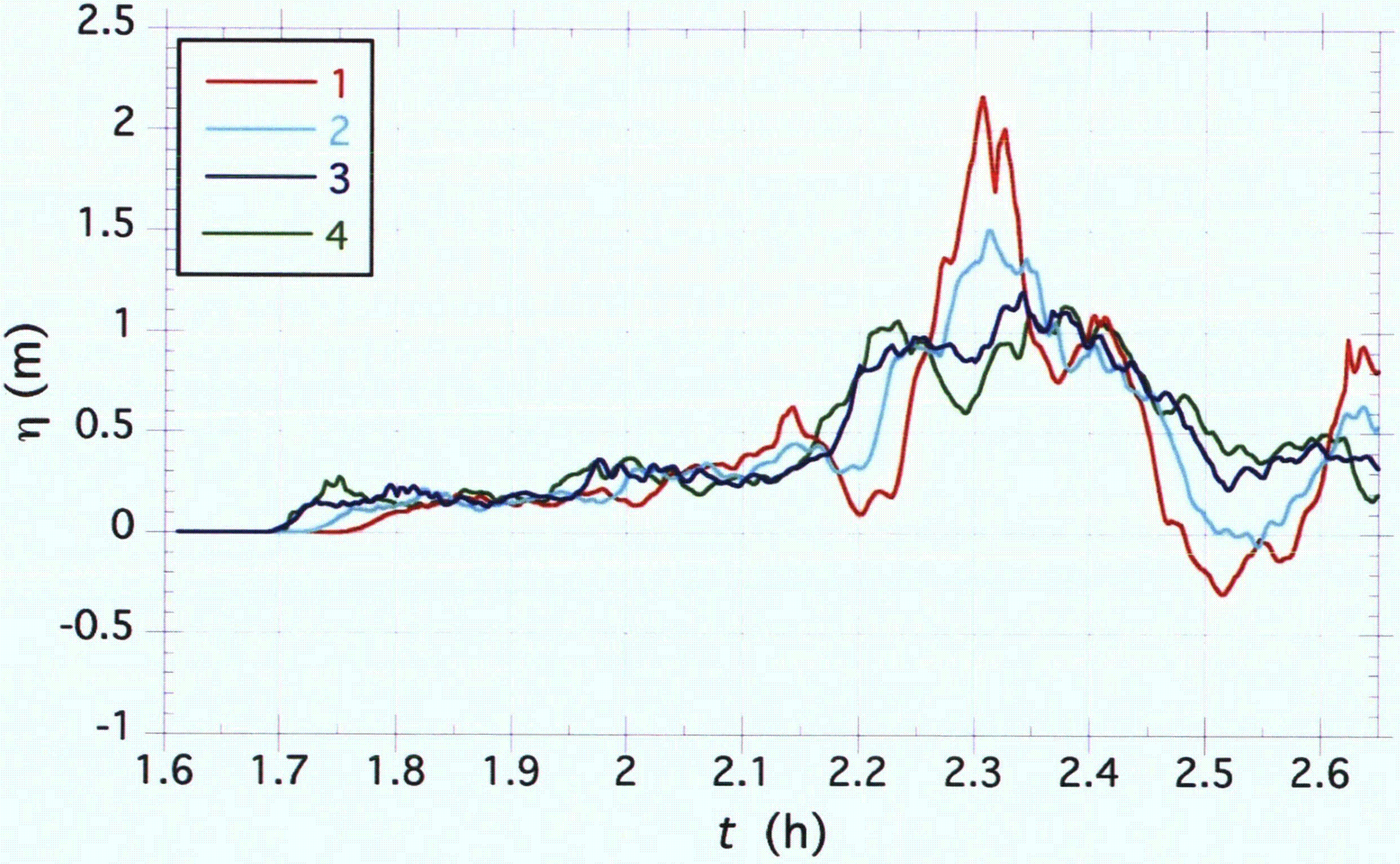

Figure 2.6-25: CurritProxy SMF source. Maximum water surface elevation (color scale in meters; referenced to 3.23 ft NAVD88) computed in the "10" meter near-field local grids, centered around the MPS site (marked by a yellow triangle). Locations of stations 1 and 2 are also noted.